A Mathematical Model of Volcanic Plumes

Submitted to the Institute of Natural and Mathematical Sciences
in partial fulfillment of the requirements for the degree of
Master of Science in Mathematics
at

MASSEY UNIVERSITY

Albany, New Zealand

Joshua Manfred Duley

2014

A Mathematical Model of Volcanic Plumes

by

Joshua Manfred Duley

Submitted to the Institute of Natural and Mathematical Sciences
on February 27, 2014, in partial fulfillment of the
requirements for the degree of
Master of Science in Mathematics

Abstract

Volcanic plumes and the resultant tephra fallout are of significant concern to nations the world over. Several recent large-scale eruptions have caused such disruption to air traffic that huge proportions of European commerce have been severely compromised. The plumes of such eruptions exist beyond any human recourse and must simply be left to extinguish themselves in time.

Currently, separate models do exist for plume dynamics and the atmospheric transport of particles, with a mixture of qualitative and quantitative results. In this thesis we develop a mathematical model with some similarities and some differences to those already in use.

The model has its core in the conservation equations of mass, momentum and energy for the plume's driving gases and suspended particles. While these equations are non-linear and difficult (if not impossible) to solve analytically, we can solve the equations numerically using a discretisation along the central vertical axis.

Initially these equations are provided with full time-dependency, with a view to pursuing such results in the future. However, the numerical results contained here are limited to a steady-flow model of an established and sustained, buoyant plume.

Acknowledgments

I would like to thank my supervisors, Professor Robert McKibbin and Dr Winston Sweatman, for the ongoing assistance, encouragement and guidance over my year of MSc study. As well as Massey University for supporting my work with a Masterate Scholarship for the period of the project. In addition to these two individuals I would also like to thank all of the educators who have endured me throughout my formal education, chiefly those who instilled a passion for mathematics within me.

I would like to thank my grandfather, Selwyn Caplan, for his lifelong dedication to formal education and the inspirational example that he has set. Finally I would like to thank my family and friends for the ongoing support and understanding that they have provided.

Cover Image: photograph taken from the International Space Station of the Mt Cleveland Eruption, Alaska (May 2006). Image courtesy of the Earth Science and Remote Sensing Unit, NASA Johnson Space Center.

Contents

List of Figures

List of Tables

Notation

Due to the large volume of notation needed in this work, ambiguity exists in the meaning of some terms. However, the context in which the symbology is used is sufficient for a distinction to be made, and throughout this thesis notation is clarified as it is introduced.

Lower case

a	m s^{-2}	Acceleration
c_V	J kg^{-1} K^{-1}	Specific Heat at constant volume
c_P	J $kg^{-1} K^{-1}$	Specific Heat at constant pressure
dZ	m	Height of a small horizontal section of plume
h	J kg^{-1}	Specific Enthalpy
k	$-$	Plume-atmosphere interface coefficients
m	kg m^{-1}	Mass per unit height
n	mol m^{-1}	Number of moles per unit height
p	Pa	Pressure
p	$-$	Proportion of particles in the sloped region of a section of plume
$q_\diamond$	$\diamond$ s^{-1}	Flux of subscript quantity
r, ϕ, z	m,rad,m	Cylindrical co-ordinates
t	s	Time
u	J kg^{-1}	Specific Internal Energy
u	m s^{-1}	Radial velocity component
v	rad s^{-1}	Rotational velocity component
w	ms^{-1}	Vertical velocity component
y	m	Difference in radius across plume section
x, y, z	m	Cartesian co-ordinates

Upper case

A	m^2	Cross sectional area
A	$-$	Suzuki constant
B	m	Radial thickness of a plumes boundary layer
C_D	$-$	Drag coefficient
E	J	Energy
$E_\diamond$	ms^{-1}	Exchange speed at the plume boundary.
		The entrainment speed is given no subscript.
F	N	Force
H	m	Maximum plume height
L	$\mathrm{K\ m}^{-1}$	Temperature lapse rate
L	m	Length scale
J	$\mathrm{kg\ s}^{-1}$	Dispersive flux
M	$\mathrm{kg\ mol}^{-1}$	Molar mass
N	s^{-1}	Brunt-Viäsälä frequency
N	#	Number of particle cohorts
P	m	Perimeter
R	m	Plume radius
R_e	m	Plume radius at the vent
Re	$-$	Reynolds number
RH	$-$	Relative Humidity
R_0	$\mathrm{J\ K}^{-1}\mathrm{mol}^{-1}$	Universal Gas Constant $:= 8.314$
S	$-$	Functional particle distribution given by Sparks *et al.* (1997)
T	K	Thermodynamic (absolute) temperatue
V	m^3	Volume
$\overline{W}$	$-$	Dimensionless velocity
Z	m	A given, fixed altitude

Greek

Δ	$-$	Numerical step
ϕ	$^\circ$	Angle about vertical axis
ψ	m	Radius of boundary layer
θ	$^\circ$C	Temperature (Celcius)
$\rho_\diamond$	kg m^{-3}	Concentration or bulk density of subscript component
ν	m^{2}s^{-1}	Kinematic viscosity
μ_p	kg	Mass of a single particle
μ_ϕ	kg	Mean
σ	kg m^{-3}	Intrinsic density
σ_ϕ	$-$	Variance
ω	$-$	Specific humidity
ζ	m^{-1}	Suzuki release distribution

Bold Font

$\mathbf{a}$	m s^{-2}	Mean acceleration
$\mathbf{u}$	m s^{-1}	Mean velocity
$\mathbf{x}$	m	Spatial location
$\mathbf{F}$	N	Force vector

Sub/Sup-Scripts, Prefaces

a	Dry air
c	Volcanic gases
e	Denotes value at vent
f	Frozen water - ice
g	Plume gases
j	Particle cohort index
l	Liquid water
$m\diamond$	Mass of component $\diamond$
m	Total plume mass
p	Particle
s	Pertaining to the particle latency
v	Water vapour
w	Total water
E	Energy
E	Extrainment
L	Denotes value at the plume apex
R	Re-entrainment
T	Terminal velocity
H_2O	Regarding a water molecule
CO_2	Regarding a CO_2 molecule
X	Extrainment
atm	Atmospheric
env	Envelope - plume's immediate boundary
max	Maximum value attainable over domain
$3w$	Triple point of water
0	Boundary condition
$\diamond$	Denotes an unknown variable to be referenced

Chapter 1

Introduction

1.1 Background and Research Motivation

Volcanic eruptions can cause massive damage and disruption to towns, cities and commerce routes. Particles transported as high as the stratosphere during eruptions encounter lateral air currents orders of magnitude greater than the terminal velocity at which they settle resulting in heavy ash fall occurring a considerable distance from the source. As a result ash plumes cannot be considered a localised phenomena, despite volcanic activity being more probable in certain regions. In saying that, with information regarding areas of high volcanic activity and the incorporation of sufficiently accurate weather forecasting an increasingly accurate model for ash columns would be invaluable.

As an example the Icelandic volcano Eyjafjallajökull underwent an eruption, officially lasting from March through October 2010, closing the majority of European airspace for six days (15th − 20th April) on account of the resultant ash cloud. Over 100,000 flights were cancelled, with approximately ten million passengers affected, at a cost of USD$1 billion to the airline industry alone. The wind conditions leading to atmospheric drift of the Eyjafjallajökull plume did play a significant role in the fallout. The role of cross-winds are beyond the scope of this thesis. However, compiling a simpler model will bring us closer to a complete picture and so, it is prudent to identify what is perhaps the most expensive eruption encountered by the modern world.

As the most significant underlying mechanism for ash transport, volcanic plumes must be clearly understood if we ever hope to continue to operate through times of activity. In accordance with its importance in both the modern and ancient world there has been academic interest in the problem.

Fortunately, in spite of difficulties surrounding taking direct measurements of eruptions, we do have a great deal of information regarding the magnitude of the majority of eruptions occurring in recent history, including data such as the explosive force of eruptions and chemical composition of magma and the volcanic gas mixture. This allows the comparison of any models generated against past eruptions, validating conclusions made. In addition to physical data about eruptions; the science of thermo-fluid dynamics is well established and by implementing known principles we can be assured of the plausibility of models generated.

As an aside, much of the following work either does not distinguish between particle and gas velocities or masses, or even include the particle related variables in the model. Therefore, in unifying the notation, variables with the subscript m or those without a subscript, denote those variables values for the whole plume mixture at the given co-ordinate(s). For example the variable $w(z)$ as opposed to $w_g(z)$ or $w_p(z)$ represents the velocity of the total plume mixture at height z, approximated to be equal for both gases and particles.

1.2 Literature Review

Prior mathematical consideration of volcanic plumes has typically taken one of two approaches. The simpler is a functional consideration of empirical data useful for confirming mechanical models. The second approach is the derivation of these mechanical models, which are the main focus of this thesis. An excellent summary of work done prior to 1997 of models for volcanic plumes can be found in "Volcanic Plumes" by Sparks *et al.* (1997), and it is from within this text that a great deal of inspiration is taken. In addition to a range of empirical results, Sparks *et al.*, present several facets of a set of conservation equations, the collection of which give a viable basis from which to proceed. More recent work by Mastin (2007) has taken a summary of results presented in Sparks *et al.*, and developed the Plumeria package which simulates an established steady flow plume attempting to imitate a sustained Plinian eruption. Robert McKibbin (2012) compiled an unpublished summary of such a model (received through private communication) which, by the addition of more state variables to the work of Sparks *et al.,* exhibits a greater level of complexity. It is necessary to derive further equations to be able to run simulations with McKibbin's increased number of variables. Within the context of the conservation equations, all of the above sources draw on results given by Woods (1988,1993). Complex meteorological models exist for the state changes of water suspended in the atmosphere; of note is the work of Khairoutdinov & Randall (2003) as used by Mastin. However a simpler model, as described in Chapter 4, is felt to be sufficient at the present time.

A highly influential paper by Suzuki (1983), provides a concise and computationally inexpensive, equation describing particle fallout derived from basic assumptions on the internal plume model and empirical data. Bursik *et al.* (1992) describe a mechanical model for particle exchange between the plume and atmosphere not included in the summaries of McKibbin (2012) or Mastin (2007). It is an interesting advancement of the mechanical model and a similar, albeit distinct, derivation is carried out later in this thesis.

1.3 Research Objective

The following research has been undertaken to develop a simple mathematical model for heated gas columns, with the chief focus being a column generated by volcanic events. In doing so we present a mechanistic theory of volcanic ash convection which we hope to later incorporate into a larger model for atmospheric transportation. Upon identification of a model we will endeavour to generate solutions for a particle fallout profile. As a secondary objective we aim to be in a position to comment on the significance of various contributing dynamics.

In our attempts to describe various components mathematically, several approximations have been made leaving some aspects of our model more rigorous than others. Because of limitations in the direct measurement of volcanic plumes at this time, it is appreciated that a large number of the modules in this model leave room for further investigation. It is hoped that in time this model may exist as a framework for which modules can be substituted in and out with successive improvement and refinement over time.

Much of the modelling in this thesis has been done with further extensions in mind. It is hoped that not only modules considered herein undergo future investigation, but that new modules and aspects can be introduced. However, in the vein of simplicity the scope of the project has been limited to a small subset of atmospheric and eruptive conditions. We do not consider complications in the atmosphere such as wind, cloud cover or any other time-dependent conditions. The most significant restriction lies in assuming that a plume exists a period of time after the initial venting such that the column can be considered an established steady flow within the atmosphere and sufficiently buoyant so that plume collapse is avoided. Sustained buoyant plumes and collapsed plumes leading to pyroclastic flow, can be separated into two distinct regions in the qualitative phase space of volcanic plumes of which we restrict ourselves to a single region.

Whilst there are known limitations in the modelling process, assumptions are made in the

analytical modelling, and approximations in numerical solutions. The resultant inaccuracies are insignificant in the light of measurement of parameters and eruption conditions. In addition to those made above, assumptions and approximations are stated where made throughout.

1.4 Methodology

As indicated the objective of this thesis is to establish a simple mathematical model for a volcanic plume as a mechanism for the transport of suspended particles and their subsequent fallout. Taking a fluid continuum, similar to an explosive jet at the base of the column; followed by a buoyant body of heated gas prior to exhaustion of the plume at its maximum height. Conservation and advection-dispersion equations are commonly used for such situations and the work that follows builds on that employed in Sparks *et al.* (1997), Mastin (2007), and McKibbin (2012). The qualitative model used in much of the literature and in this thesis assumes that aside from volcanic material introduced to the plume at the vent, the only exchange of mass occurs as a result of entrainment or a particle fallout/re-entrainment cycle on the plume boundary.

Advection-dispersion equations, if simple enough, can have analytical solutions. However in the work that follows the non-linearity of equations restricts us to numerical solutions. Numerically solving the model for discrete cohorts of particles will give indications of a fallout profile. Unfortunately, due to the same non-linearities these solutions cannot be superposed onto one another. Therefore, for increasingly rigorous solutions with large variability in particle categorisation, simulations must be run with the whole spectra of particle characteristics simultaneously. This range of categorisations has not be done in this thesis. In spite of that, sufficient results are gathered for us to generate indicative solutions.

1.5 Thesis Overview

This thesis represents a summary of several influential concepts and models describing the fluid and thermodynamics of ash clouds as a particular phenomenon of Plinian volcanic eruptions. Chapter 2 discusses some basic assumptions made and highlights our modelling process' roots in established volcanic theory. Here we cover the major sources of mass for the plume, sequentially covering the venting of volcanic material, assumptions on its passage into the atmosphere, the resultant entrainment of atmospheric gases, and the appropriate

correlations for the state variables as they exist outside of the plume. In concluding the chapter we shift focus from the contents of the plume to the time scales of an eruption.

Chapters 3 and 4 detail models on the dynamics of an established, buoyant volcanic plume as well as some extensions of these results representing research done during the span of this project. Chapter 3 considers the exchange of tephra at the boundary of the plume. Chapters 4 discusses the development of the internal model which acts as the vertical transport mechanism advecting any retained ash particles. Supplementing Chapter 3 are two fallout models derived from quite distinct observations which will allow for more rigorous qualification of our results.

Chapter 5 presents the steady state model, as well was any final assumptions made in the commission of the model to computer simulation. From there, implementing indicative boundary conditions on the vent we are in a position to seek solutions to our set of differential equations.

Drawing final conclusions in Chapter 6 we re-iterate distinctions made in this thesis from the literature and potential for the expansion of this important field of study.

Chapter 2

Preliminaries

This chapter outlines some basic approximations made in the modelling process, discusses the context of our model, and explains how the model fits into the modern understanding of Plinian eruptions.

2.1 Plume shape and the umbrella region

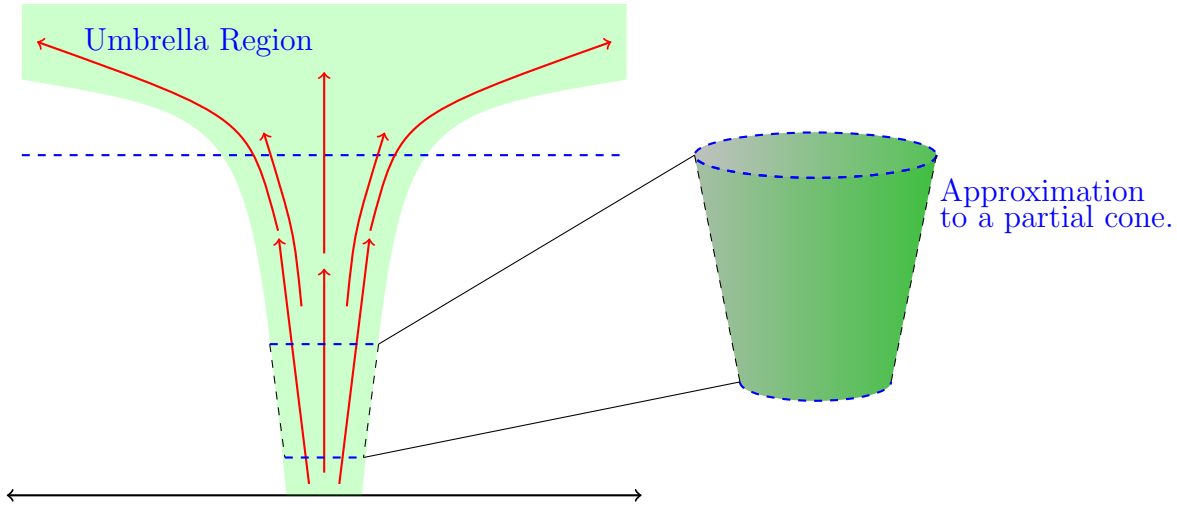

Figure 2-1: A schematic illustration of the umbrella region of ash clouds and a partial cone approximation to a thin slice.

Plumes and ash clouds make for striking images both for their magnitude and stark contrast to their often softer surroundings. The sharp definition seen in plumes is due to the relatively high particle concentrations in volcanic plumes and the billows seen on the surface give an indication of the turbulent environment within a plume. Unfortunately this level of detail is impossible to recreate with the simple tools we intend to implement and so the plume's edge is taken as a time-averaged surface, which gives a smooth profile. We can make another simplification, illustrated in Figure 2-1, taking thin horizontal slices of plumes to have trapezoidal vertical cross-sections which, when rotated about a central axis, are similar to partial cones. In addition to these local shape characteristics, columns produced in Plinian eruptions will have what is known as an umbrella shape, similar to mushroom clouds seen in atomic detonations. As plumal gases begin to lose their kinetic energy, near the apex of the plume, they slow down rapidly causing an accumulation of mass. As more gas rises, it forces lateral displacement of volume, seen as a rapid radial expansion in the plume generating what is commonly known as the umbrella region.

2.2 Plume content

In volcanic eruptions, vast amounts of various chemicals are ejected into the atmosphere. Halmer *et al.,* (2002) provides a compilation of samples from volcanic events over the past 100 years and from these we have a clear insight into the composition of plumes. The ratios of components do vary between eruptions but there are trends carried across most events.

Of particular note is the prevalence of water and carbon dioxide in contrast to other trace elements. Occasionally sulfur dioxide will make up a significant part of the lower plume reaches. However, for the sake of simplicity and in light of the fact that this is only an occasional scenario, it is sufficient to make the approximation that as it is vented a plume is composed of water vapour (at $40 - 99\%$ by volume) and the remainder carbon dioxide. In the interests of comparison to specific eruptions the reader is invited to substitute specific values in lieu of the generality presented in this thesis.

Figure 2-2: An aerial image of the May 18, 1980, Eruption of Mt St Helens, Washington. Courtesy of the U.S. Geological Survey.

2.3 Decompression

Volcanic and hydrothermal plumes are caused by rapid expansion of gases exsolved from subterranean magma as is brought to the surface. This degassing of the magma can cause a volumetric expansion of several orders of magnitude over very short periods of time and distances. Within a restricted conduit the gas is pressurised to the order of $10 - 100$ atm. As described by Woods & Bower (1995), when these gases are vented at the surface, meeting with the relatively low pressured atmosphere the plume undergoes decompression expanding laterally and accelerating vertically away from the vent. This leaves two possible eruption conditions for our model. Either we can begin at the vent incorporating the known results of decompression, or slightly above the vent under the assumption that the plume has had sufficient time to decompress. In either situation beyond the point of decompression the plume is assumed to be isobaric to the atmosphere. The results discussed in the above paper give a very detailed analysis of various situations such as venting within or outside of a crater and column collapse. However the main focus of this thesis is the dynamics of an established plume. In the light of which and for the sake of simplicity, we will be considering a decompressed plume typically measured from a height of a few vent radii above the surface. In doing so we do not severely limit the scope of this thesis, as it is simply shifting the focus away from excessively specific initial conditions for which precision is not absolute in real world measurement. In the pursuit of simulation it is sufficient to concatenate a separate decompression script run in anticipation of the model presented in this thesis should the reader require it. Within the thesis in terms of terminology 'venting' or 'vent altitude' or similar terms indicate the lower boundary of the column, z_e, measured from sea-level, from which simulations are run.

2.4 Gas Velocity and Turbulence within the Plume

With the obvious difficulties surrounding measurements on the interior of plumes the velocity profile is typically assumed to be either Gaussian, with the plume travelling faster at its core or, more simply, a 'top-hat' model, that is with uniform velocity for a given altitude within

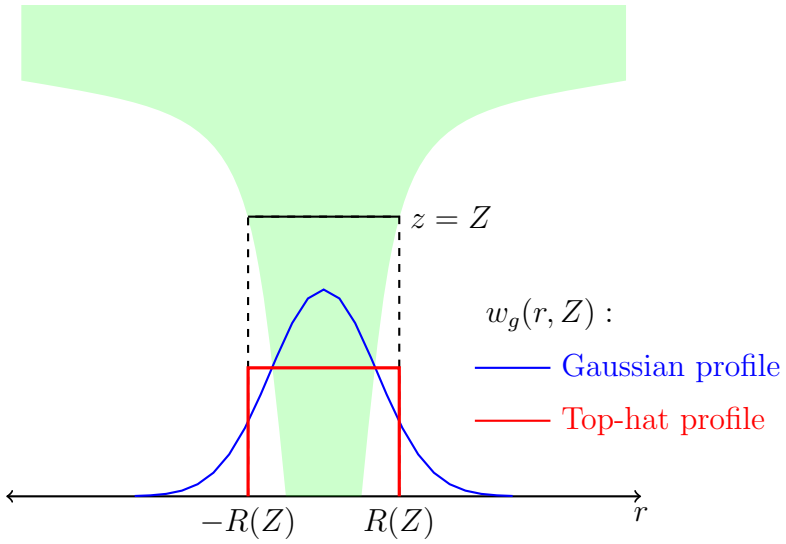

Figure 2-3: A schematic illustration of the Top-hat and Gaussian velocity models, indicating their relation to the plume boundary at height $z = Z$.

the plume and the atmosphere stationary. These assumptions are explored experimentally by Solovitz & Mastin (2009) and the approach is used in modelling plumes regularly, including work by, Sparks *et al.* (1997), Mastin (2007) and McKibbin (2012) as a few examples. In this instance it is assumed that all horizontal cross-sections of the plume are circular. If, at a later date, the introduction of a cross wind is considered, the relationship of these assumptions must be reconsidered. The top hat model can be expressed mathematically as:

$$\mathbf{u}_\diamond(r, \phi, z) = \begin{pmatrix} u_\diamond(r, \phi, z) \\ v_\diamond(r, \phi, z) \\ w_\diamond(r, \phi, z) \end{pmatrix} = \begin{pmatrix} 0 \\ 0 \\ w_\diamond(z) \end{pmatrix}, \tag{2.1}$$

over the range $0 < r \leq R(z)$, $0 < \phi \leq 2\pi$, $z \geq z_e$ where, $\mathbf{u}_\diamond$ is the plume velocity, $R(z)$ is the radius of the plume at height z, and z_e the vent altitude. Beyond the radius of a plume the atmosphere has already been assumed stationary and so we have a naturally restricted domain. This model is illustrated in Figure 2-3.

In addition to the velocity profile at a given height a significant question we need to ask

ourselves is what shape the distribution of our other dependent variables ought to take. Ultimately the turbulent dynamics are dictated by the gases which act according the Reynolds number,

$$Re = u\frac{L}{\nu}, \tag{2.2}$$

where u is a speed scale, L is a standard length scale, and ν is the kinematic viscosity. For an approximation of the kinematic viscosity, Batchelor (1967) provides a range of values, reproduced here in Table 2.1. The Reynolds number for the bulk flow of a high velocity

Table 2.1: The viscosity of dry air, at one atmosphere, over the range $-100 \leq \theta \leq 1000$ [K].

Temperature °C	Density 10^3 kg m^{-3}	Viscosity 10^{-1} kg m^{-1} s	Kinematic Viscosity 10^{-4} m^2 s^{-1}
-100	0.00204	0.000116	0.057
0	1.293	1.71	0.132
100	0.946	2.18	0.230
200	0.746	2.58	0.346
300	0.616	2.95	0.481
500	0.456	3.58	0.785
1000	0.277	4.82	1.74

plume can be approximated by taking speed and length scales at the vent, $uL = w_{ge}2R_e$ which will typically be of the order of $10^2 - 10^4$ m^{2}s^{-1}. Approximating the kinematic viscosity of a plume to be the same as dry atmosphere this gives a Reynolds number of the order of $10^6 - 10^9$, which indicates a highly turbulent environment. This high level of turbulence means we can comfortably assume that plumes exhibit a well mixed profile horizontally across their cross-sections. This allows simplification in our model's dynamics, varying along one spatial dimension, parallel to the vertical axis (z) and independent of the horizontal plane (r, ϕ). This turbulence will also mix our plume along the vertical axis through eddies and vortices within the column. However the vertical length scale will be much larger than the horizontal ($z_L \gg R(z)$) which represents a limit on eddy diameter and so substantial vertical variation is still expected.

2.5 Ballistic Trajectories and Drag

It is a rudimentary principle that, given a functional expression for the acceleration of a particle, its trajectory can be calculated by integrating through from initial spatial and velocity conditions.

$$\begin{aligned} \mathbf{x}(0) &= \mathbf{x}_0 \quad ; \quad \mathbf{u}(0) = \mathbf{u}_0 && (2.3)\\ \frac{d\mathbf{x}}{dt} &= \mathbf{u} && (2.4)\\ \frac{d\mathbf{u}}{dt} &= \mathbf{a}, && (2.5) \end{aligned}$$

Within a top-hat (one-dimensional), steady flow model, this Lagrangian system can be easily rearranged to fit the Eulerian view as seen in the conservation equations of the following chapter.

$$\begin{aligned} \frac{dz_p}{dt} &= w_p \\ dt &= \frac{dz_p}{w_p} \\ \frac{dw_p}{dt} &= a_p \\ \frac{dw_p}{\left(\frac{dz_p}{w_p}\right)} &= a_p \\ w_p \frac{dw_p}{dz_p} &= a_p. && (2.6) \end{aligned}$$

If we don't need to determine the height of a particular particle we can remove the subscript from z_p.

$$w_p \frac{dw_p}{dz} = a_p = \frac{F_p}{\mu_p}. \tag{2.7}$$

Assuming that the only significant forces acting on them are drag, F_D, and weight, F_g, we can derive the acceleration they experience according to Newton's second law,

$$\mu_p a_p = F_D + F_g, \tag{2.8}$$

where μ_p is the average mass of a particle. For high-velocity flow, Green & Perry (2008, p. 6-51 to 6-52) express the drag force on a particle as,

$$F_D = \frac{1}{2}\rho_g u^2 C_D A_p, \tag{2.9}$$

where u is the relative velocity between the fluid and the particle, C_D the drag coefficient, and A_p the area of the particle projected onto a plane normal to the flow. Assuming that the particles are spherical, Green & Perry go on to express the drag coefficient as a function of the Reynolds number,

$$C_D = \begin{cases} \frac{24}{Re} & Re < 0.1 \\ \frac{24}{Re}\left(1 + 0.14Re^{0.70}\right) & 0.1 < Re < 1000 \\ 0.445 & 1000 < Re < 350000 \\ - & 350000 < Re < 1 \times 10^6 \\ 0.190 - \frac{8\times 10^4}{Re} & 1 \times 10^6 < Re \quad . \end{cases} \tag{2.10}$$

For $350000 < Re < 1 \times 10^6$, the drag coefficient undergoes what is called a drag crisis, where the coefficient drops rapidly between 0.445 and 0.110. This rapid change is heavily influenced by the surface roughness of the particle and so a value is not given in the text. The Reynolds number for the bulk flow in volcanic plumes, as covered in Section 2.4, is of the order $10^7 - 10^8$, however in the context of drag over a particle we are operating on a different scale. Considering the diameter of suspended particles Sparks et al. (1997) provides an upper limit of 1 mm, or 10^{-3}m. The relative speed between the gas and particles is of the order of 10^1 m s^{-1}. This gives us a Reynolds number of $Re \simeq \frac{10^1\, 10^{-3}}{10^{-4}} = 10^2$, and corresponding drag coefficient of approximately $C_D \simeq 1.084$. The value of the drag coefficient is highly influential on particle fallout profiles and so variation in this value will have a visible impact on the results shown in Chapter 6.

2.6 Atmospheric Conditions

The atmospheric pressure profile is taken (Portland State Aerospace Society, 2004) as a function of altitude:

$$\begin{aligned} p_{atm} &= p_0 \left(1 - \frac{zL}{T_0}\right)^{gM_{atm}/R_0 L} \\ &= 101325 \left(1 - \frac{z}{44330}\right)^{5.26} \qquad \text{[Pa]}, \end{aligned} \tag{2.11}$$

where p_0 is standard atmospheric pressure at sea level, L the temperature lapse rate, T_0 standard temperature at sea level, g gravitational acceleration, M_{atm} the molar mass of dry atmospheric air, and R_0 the universal gas constant.

While the atmospheric temperature profile can vary considerably we have taken a simple, piecewise linear approximation dependent on the altitude and applicable atmospheric zone. Volcanic plumes are typically contained in a maximum altitude of 48km. Up to an altitude of 55 km, the atmospheric temperature has been taken as the following approximation of instantaneous data (Handbook of Geophysics and the Space Environment, 1985),

$$\theta_{atm}(z) = \begin{cases} \theta_0 - 6.5\frac{z}{1000}; & 0 \leq z \leq 11,500 \text{ m} \\ \theta_0 - 74.75; & 11,500m < z \leq 20,000 \text{ m} \\ (\theta_0 - 74.75)\frac{48000-z}{28000}; & 20,000m < z \leq 48,000 \text{ m} \\ 0; & 48,000m < z \leq 55,000 \text{ m} \end{cases} \qquad [^\circ\text{C}] \tag{2.12}$$

$$T_{atm}(z) = \theta_{atm}(z) + 273.15 \qquad \text{[K]}. \tag{2.13}$$

Standard atmospheric pressure is limited to 101325 Pa (1 atm), and by Section 2.3 this limits the pressure of gases both inside and out of our plume. For pressures in this range, gases can be taken to act as ideal gases. From this, atmospheric density can be calculated by the

ideal gas equation,

$$\begin{aligned} p_{atm}V &= nR_0T_{atm} \qquad (2.14) \\ \frac{V}{n} &= \frac{R_0T_{atm}}{p_{atm}} \\ \frac{M_{atm}}{\rho_{atm}} &= \frac{R_0T_{atm}}{p_{atm}} \\ \rho_{atm} &= \frac{M_{atm}p_{atm}}{R_0T_{atm}}. \qquad (2.15) \end{aligned}$$

We must also take into account the humidity of the atmosphere. Aside from water, atmospheric composition can be taken to be fairly standard but humidity will vary considerably depending on a range of factors. Relative humidity is defined as $0 \leq RH = \frac{p_{v,atm}}{p_{v,sat}} \leq 1$ where $p_{v,atm}$ is the partial pressure of water vapour in the atmosphere and $p_{v,sat}$ the saturation point. The relative humidity can ultimately be selected to match any specific condition. Within this thesis we have taken it as $RH = 0.9$. The specific humidity, ω, which represents the ratio of entrained water vapour to entrained dry atmosphere, has the form,

$$\omega = \frac{M_{H_2O}}{M_a}\frac{p_{v,atm}}{p_{atm} - p_{v,atm}}. \qquad (2.16)$$

2.7 Entrainment

Entrainment of fluids is a widely-understood phenomenon that occurs in any turbulent environment where one fluid passes over another. Occurring as a result of shear forces and turbulent eddies, entrainment is the mechanism by which one body of fluid passing over another draws additional flow into its stream. The speed at which this occurs is typically taken as proportional to the difference in the velocity of the two fluids,

$$E(w_g) = k_E|w_g|. \tag{2.17}$$

In terms of the geometric depiction of entrainment, the entrainment speed $E(w_g)$ is taken orthogonal to, and orientated towards, the central axis. The parameter k_E can, in the simplest model, under a fixed flow type, be taken as a constant. Differentiating between the dynamics of a driven jet and buoyant plume, Sparks *et al.* (1997) gives two possible values,

$$k_E = \begin{cases} 0.06 \quad ; & \text{Explosive jets} \\ 0.09 \quad ; & \text{Bouyant plumes} \end{cases}$$

Explosive jets characterise a gas-thrust region where large velocity and large deceleration is experienced in a plume. Beyond this, there exists a convection region where the plume is buoyant with respect to the surrounding atmosphere. A plume will only exhibit jet-like behaviour for a short period immediately after venting and so, in this simple case, it is better to take $k_e = 0.09$. Alternatively k_E can be defined piecewise-constant over the two regions for a more detailed model. The most complex representation (as discussed by Sparks *et al.*, 1997, seen originally in Woods, 1988) is a functional expression mirroring the effects of changes in the relative difference between the bulk plume density, ρ_m, and atmospheric density, ρ_{atm}. It is this final relationship that is used in the results of this thesis,

$$k_E = 0.09\sqrt{\frac{\rho_m}{\rho_{atm}}}. \tag{2.18}$$

More indepth models are discussed in Fischer (1979) and Kaminski *et.al.* (2005) and for small scale plumes with high degrees of accuracy in the measurement of parameters it may

be necessary to go to the level of detail seen there. However for volcanic eruptions the level of uncertainty is such that we can be satisfied by the relationship in Equation (2.18).

2.8 Particle Exchange

As the plume gases rise, drag between the plume and the atmosphere will cause atmospheric gas to be entrained into the plume where it will quickly mix into the existing components. Whilst entrainment is a significant source of mass for the plume, the frictional effects are negligible compared to the energy and momentum a plume contains.

This entrainment of gas works against the flow of particles being extrained from the plume by exerting an inward drag onto the particles. If this force is sufficiently large then we may have the re-entrainment of particles whereby they rejoin the main advective column. Reducing this description to the situation indicated in Figure 2-4 and allowing more complex paths to be overlooked we can derive a simple equation describing the particle exchange on the plume boundary. Particle exchange is explored quantitatively in Chapter 3.

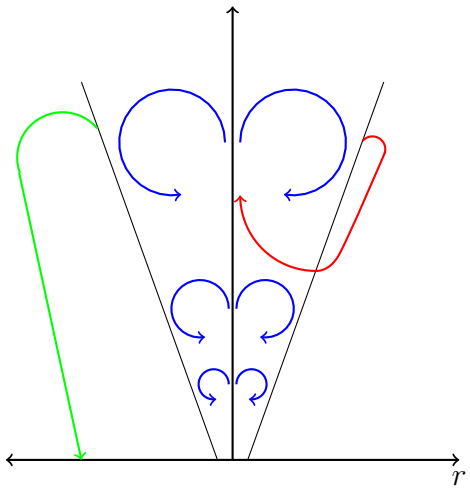

Figure 2-4: An illustration of the significant mechanisms in plumal particle transport, incorporating extrainment with fallout (green), extrainment with re-entrainment (red), and the limit on eddy size acting to promote dispersion within the plume (blue).

2.9 Time Dependency

Operating a dynamical system in both spatial and temporal dimensions markedly increases the complexity of the system and the difficulty when it comes to finding solutions. Radar observations from the Mt St Helens eruption in May 1980 (Harris *et al.,* 1981) show a level of consistency in the plume height, from which we can argue that for similar eruptions a steady state model may be appropriate.

Sparks *et al.* (1997) correctly note that for a plume to be considered in steady state the buoyancy flux at the vent must remain constant for a period of time greater than the order to which it takes material to travel from the vent to the height of the column. Going on to approximate this time scale to be of the order of $\frac{1}{N}$ where N is the Brunt-Viäsälä frequency given as,

$$N^2 = -\left(\frac{g}{\rho_{atm}}\frac{d\rho_{atm}}{dz}\right)\Bigg|_{z=0}. \tag{2.19}$$

This gives $\frac{1}{N}$ to be in the order of 2 to 3 minutes. One could then conservatively say that a plume with a steady vent flux for 20 minutes would behave as if in a steady state.

Time scales as seen above with the Mount St Helens eruption are therefore well beyond the necessary criterion. Mount St Helens not being an a-typical eruption, we can conclude that modelling volcanic plumes, for restricted periods of an eruption, can accurately be done under the assumption that they are in a state of steady flow. In doing so we still take a step towards developing a full time-dependent model even if in the meantime this prevents modelling of the transition between a steady flow and eruptive surges as seen in Table 2.2 at times 0845, 1158, and 1705.

For the sake of generality, we will conduct our modelling with full time dependency, however the equations are reduced to steady state before solving.

Table 2.2: Radar measurements of the Plinian column and estimated magma emissions during the May 18, 1980 Mt St Helens eruption. Immediately after the initial vent breach, the plume ascended beyond the capability of radar measurement and so the exact plume height is not available for the first reading at 0845.

Time	Plume Height [km]	Estimated Emission rate of dense dacite[10^3 m^3s^{-1}]
0845	>22	>23.0
0915	12	2.0
0938	12	2.0
1100	13	2.5
1158	15	5.0
1255	11	1.5
1330	13	2.8
1500	13	2.8
1605	14	3.8
1705	17	8.3
1800	5	0.06

Chapter 3

Particle Exchange

Particle transport in a plume can be modelled effectively at a variety of levels of detail. The most basic seen in the literature takes particles to be wholly contained up to the point at which they become neutrally buoyant. Adding complexity to this provides particles falling from the plume due to a combination of dispersive and advective factors with consideration of re-entrainment. Alternatively distributions are provided by Sparks *et al.* (1997), Suzuki (1983) and McKibbin (2008) that describe (as a function of vent conditions) the distribution of particles both inside and outside of the plume. The following chapter discusses the dynamics for a single particle class. Assuming that particle interaction is limited, with regards to post-venting fragmentation and conglomeration, then the generalisation to distinct particle classes can simply be done by the addition of the appropriate indices.

3.1 Slice dynamics

Accepting the conservation of flow of volcanic debris, if particles are retained up to the point of neutral buoyancy, z_{NB}, then we can express the situation with the differential equation:

$$\frac{\partial m_p}{\partial t} + \frac{\partial q_{mp}}{\partial z} = -\delta(z - z_{NB}) q_{mp}, \tag{3.1}$$

where $\delta(z)$ represents the Dirac-delta function or delta distribution. This is the most simple of the advection models for mechanistic fallout. The point of neutral buoyancy represents

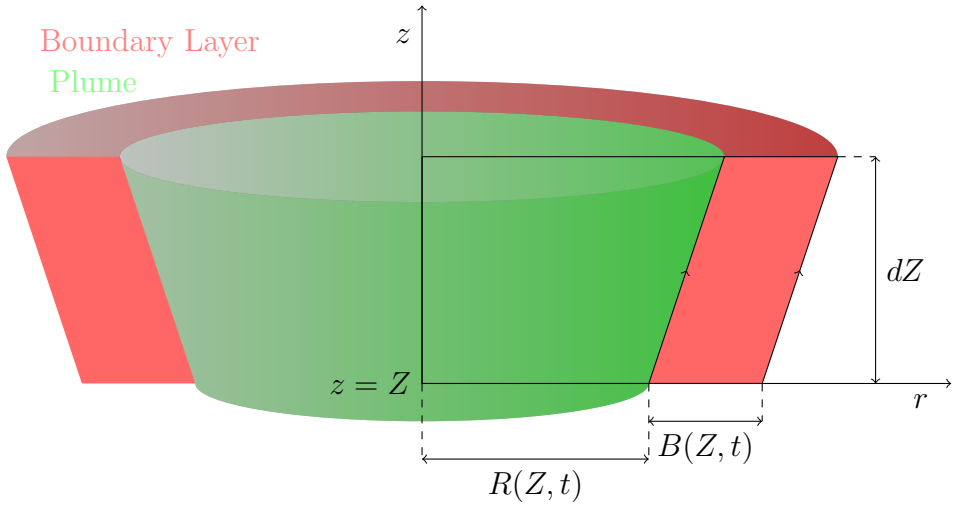

Figure 3-1: An approximation to a horizontal slice of plume with cylindrical coordinates overlain

the altitude at which the drag force, and weight of a particle are balanced. It can be analytically shown that this equation represents the total conservation of particle flux up to height $z = z_{NB}$, followed by total fallout at this height; explicitly this can be written as,

$$q_{mp} = \begin{cases} q_{mpe} & z \leq z_{NB} \\ 0 & z > z_{NB} \end{cases} . \tag{3.2}$$

If we assume that particles are lost from the plume continuously as the column rises a more interesting model develops. To investigate this situation let us consider a horizontal slice of plume of thickness dZ with its base at altitude Z. Let us also define a boundary layer of thickness $B(z,t)$ so that the plume and boundary layer are within a distance of $R(z,t) + B(z,t)$ from the centre of the plume at $r = 0$, to be made distinct from the atmosphere. For a sufficiently small slice the plume edge is approximately linear; this construction can be seen in Figure 3-1. The plume radius excepted, let us consider all other state variables to be constant with respect to their height within the slice, and taken to an average across the thickness of the slice.

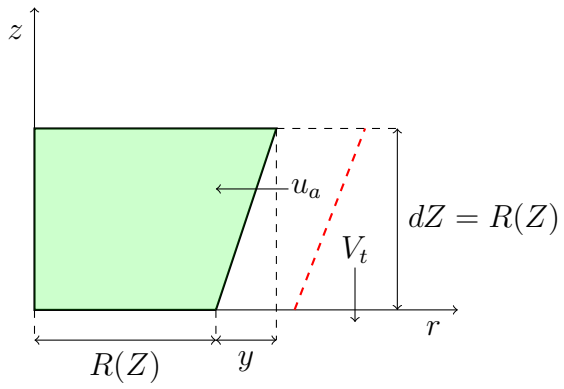

Figure 3-2: The schematic figure representing a plume section as used by Sparks *et al.* (1997). The additional variables mentioned u_a, V_t, y, dZ represent an indicative inward flow rate of particles across the plume boundary, the terminal velocity of particles in the atmosphere, the change in radius of the plume across our section, and the height of the section respectively.

3.1.1 The fallout model of Sparks *et al.* (1997 - Chapter 14).

Proposing successively more complex models for particle exchange, Sparks *et al.* (1997) began with no particle loss before neutral buoyancy through to the introduction of fallout and re-entrainment terms where the ultimate result (notation revised) is:

$$\frac{dq_{mp}}{dz} = -\frac{q_{mp}V_t}{w}\frac{p}{R} + \frac{k_R q_{mp} u_a}{w}\frac{p}{y}, \tag{3.3}$$

where $\frac{p}{R}$ is the proportion of particles per unit height in the sloped regions of the plume which are liable to fall out from the plume; y, the difference in radius across the control section; u_a, a radial inflow speed; and V_t, the terminal velocity of a particle in the atmosphere. It is derived within the framework illustrated in Figure 3-2, with the specification of $dZ = R$. A single plume velocity w is used by Sparks *et al.,* as opposed to a gaseous-particle distinction.

3.1.2 A geometric argument of Bursik *et al.* (1992).

In the context of Subsection 3.1.1, Sparks *et al.* (1997) have quoted a result from Bursik *et al.* (1992) giving $p = 0.266$. Unpacking the original paper Bursik *et al.,* provides a more detailed result that is worth introducing here. Taking the construction in Figure 3-2, the proportion of particles situated further from the central axis than the radius at height $z = Z$,

are considered liable to fallout. Bursik *et al.* approximated this as the ratio of the change in cross sectional area to the average cross sectional area. In the following equation the radius, R, is measured at height $z = Z$, and the thickness of the section is taken to be equal to the radius, $dZ = R(Z)$. This may in fact result in a rather thick slice.

$$p = \frac{\pi\left(R + dZ\frac{dR}{dz}\right)^2 - \pi R^2}{\frac{1}{2}\left(\pi\left(R + dZ\frac{dR}{dz}\right)^2 + \pi R^2\right)} \tag{3.4}$$

$$= \frac{\pi\left(R + R\frac{dR}{dz}\right)^2 - \pi R^2}{\frac{1}{2}\left(\pi\left(R + R\frac{dR}{dz}\right)^2 + \pi R^2\right)} \tag{3.5}$$

$$= 2\frac{\left(1 + \frac{dR}{dz}\right)^2 - 1}{\left(1 + \frac{dR}{dz}\right)^2 + 1}. \tag{3.6}$$

In addition to this, Bursik *et al.,* took the entrainment rate to be, $k_E = 0.1$; and the plume slope as $\frac{dR}{dz} = \frac{6k_E}{5}$, giving $p = 0.266$.

3.1.3 An argument of exchange speeds

There is a clear geometric similarity between particle exchange and the entrainment mechanism, where the qualitative model can be described as the transfer of mass across an inclined boundary separating domains of differing (bulk) density for the relevant plume component. The total flux across the boundary can be expressed as the integral of the concentration flux over the length of the interface, being the perimeter of the plume, P. The product of the concentration, $\rho_\diamond$, and a speed of exchange (in the horizontal plane, orientated inwards to the central axis) gives the concentration flux at a point. In terms of particle exchange we have the concentration of particles, ρ_p and the perimeter of the plume indicating the length of the interface, P. As illustrated in Figure 3-3, let us take the exchange speed to be $E_X(w_g, w_p)$ [ms^{-1}]. Note the reflection into the horizontal plane across the plume edge gives $-E_X(w_g, w_p)\frac{dR}{dz}$ [ms^{-1}]. Integrating the concentration flux about the plume perimeter gives,

$$\frac{\partial m_p}{\partial t} + \frac{\partial q_{mp}}{\partial z} = -P\rho_p E_X(w_g, w_p)\frac{\partial R}{\partial z} \tag{3.7}$$

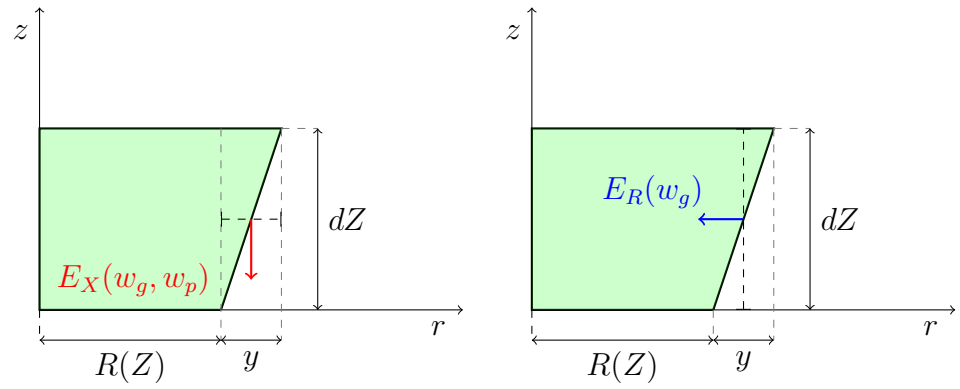

(a) (b)

Figure 3-3: The schematic plume section applied to particle entrainment and re-entrainment. Part (a) indicates the extrainment flow rate equivalent to an extrainment speed E_X across interface length y. Part (b) indicates the reentrainment flow rate equivalent to a reentrainment speed E_R across interface length dZ.

The extension of this including a re-entrainment term is,

$$\frac{\partial m_p}{\partial t} + \frac{\partial q_{mp}}{\partial z} = -P\rho_p E_X(w_g, w_p)\frac{\partial R}{\partial z} + Pk_R\rho_p E_R(w_g). \tag{3.8}$$

where $k_R\rho_p$ represents the concentration of particles in the immediate vicinity of the plume available for re-entrainment, and $E_R(w_g)$ [m s^{-1}] the re-entrainment speed. These two exchange speeds are illustrated in Figure 3-3.

This result can be reconciled to that of Sparks *et al.* (1997) by relaxing some of the assumptions made there. Altering the situation in Figure 3-2, we take a slice of plume with an arbitrary thickness, $dZ \ll R$. From there the variable y, representing the change in plume radius across our section can simply be expressed as,

$$y = \frac{dR}{dz}dZ. \tag{3.9}$$

Additionally, taking the same construction of the proportion p, as in Equation (3.4), gives,

$$p = \frac{\pi\left(R + dZ\frac{dR}{dz}\right)^2 - \pi R^2}{\frac{1}{2}\left(\pi\left(R + dZ\frac{dR}{dz}\right)^2 + \pi R^2\right)} \tag{3.10}$$

$$= \frac{2RdZ\frac{dR}{dz} + \left(dZ\frac{dR}{dz}\right)^2}{R^2 + RdZ\frac{dR}{dz} + \frac{1}{2}\left(dZ\frac{dR}{dz}\right)^2}. \tag{3.11}$$

From which we can take the significant term,

$$p = \frac{2dZ}{R}\frac{dR}{dz}, \tag{3.12}$$

$$\frac{p}{dZ} = \frac{2}{R}\frac{dR}{dz}, \tag{3.13}$$

as well as,

$$\frac{p}{y} = \frac{2dZ}{R}\frac{dR}{dz}\frac{dz}{dR}\frac{1}{dZ} \tag{3.14}$$

$$= \frac{2}{R}. \tag{3.15}$$

Subject to algebraic rearrangement; substitution of the values p and y as above; replacing the exchange speeds, V_t and u_a, by the general functions, E_X and E_R respectively in Equation (3.3); and letting Equation (3.8) tend to a steady state we have the same mathematical model in both instances.

$$\frac{dq_{mp}}{dz} = -\frac{q_{mp}E_X}{w_p}\frac{dR}{dz}\frac{2}{R} + \frac{k_R q_{mp}E_R}{w_p}\frac{2}{R} \tag{3.16}$$

$$= -\frac{m_p w_p E_X}{w_p}\frac{dR}{dz}\frac{2}{R}\frac{\pi R}{\pi R} + \frac{k_R m_p w_p E_R}{w_p}\frac{2}{R}\frac{\pi R}{\pi R} \tag{3.17}$$

$$= -\frac{P}{A}m_p E_X\frac{dR}{dz} + \frac{P}{A}k_R m_p E_R \tag{3.18}$$

$$= -P\rho_p E_X\frac{dR}{dz} + Pk_R\rho_p E_R. \tag{3.19}$$

The turbulent boundary layer on the boundary of the plume separates the core plume from

the atmosphere. Across this width of fluid, neither the assumptions made on the plume nor those made on the atmosphere apply, as it acts as a transition between the two. Assumptions that can be made about this region are that this transition acts continuously preserving boundary conditions and also that the boundary layer is thin enough that the vertical flux contained within it is negligible when compared to the bulk plume flux. Considering the application of the boundary conditions there are two distinct possibilities as seen on the two edges of this boundary layer. Figure 3-4 gives an example of these differences, it is heuristically generated, but indicates (for both Gaussian and top-hat models) the purported difference in gas velocities at the two edges and therefore the level of gaseous support suspended particles have.

This boundary layer acts as the mechanism for the entrainment of gas and its dynamics are expressed simply in Equation (4.53), with the exchange speed for gases pass through the boundary taken as a function of the plume speed, $E(w_g)$. In the same way we need a simple model describing the speed with which particles pass through the region. The distinction in vertical particle and gas velocities is made because of the settling effect gravity has on particles. However, perpendicular to the action of gravity, we assume that the particles are travelling horizontally at the same speed as the gas. This would imply then, that particles ought to be re-entrained at the same rate as atmospheric gas is entrained $E_R(w_g) = E(w_g) = k_E w_g(z)$.

For the extrainment speed, Sparks *et al.* (1997) considered fallout on the external edge, taking the value $E_X = V_t$, the terminal velocity of a particle deposited in the atmosphere. The proposed value for an extrainment model focussing on the internal edge of a boundary layer is marginally more complex. As the plume spreads out laterally, the suspended particles within it are assumed to maintain a uniform concentration across the plume at a given altitude. From this, we can approximate the speed at which the particles are spreading laterally to be equal to the speed at which the plume gases are. Implementing this result in a velocity vector diagram, illustrated in Figure 3-5, indicates on the internal edge, an equivalent extrainment rate of $E_X(w_g, w_p) = w_g - w_p = w_s$.

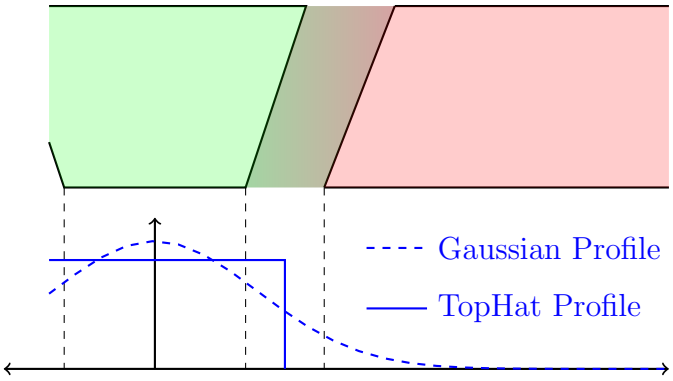

Figure 3-4: The qualitative division between the plume and the atmosphere with an exaggerated boundary layer.

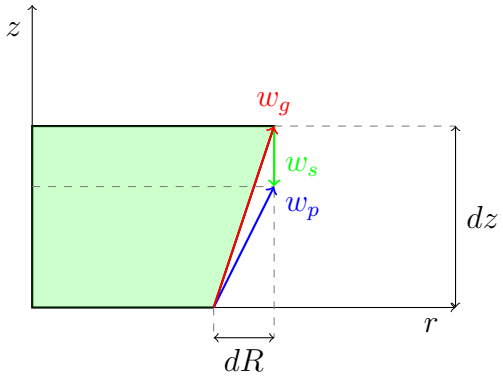

Figure 3-5: The velocity vector diagram resolving the particle extrainment rate given the lateral expansion of the plume and particle latency.

Still operating on the internal edge, we have by the continuity across it, the density of particles as they are entrained, $k_R\rho_p$, equal to that within the plume, ρ_p. This is a very simple estimate to make and certainly open to further exploration.

It is assumed that particle fallout it is non-negative; That is to say, when the re-entrainment rate is greater than the extrainment rate we take the fallout to be zero.

$$\frac{\partial m_p}{\partial t} + \frac{\partial q_{mp}}{\partial z} = 0. \tag{3.20}$$

3.2 Vertical dispersion

Eddies within a plume do not swirl solely in the horizontal plane and so it can be expected that they will act to mix the particle concentration vertically within the plume. According to Fick's law the dispersive flux, J, will be proportional to the concentration gradient,

$$J = -D_z \frac{\partial c}{\partial z} \quad [\text{kg m}^{-2}\text{s}^{-1}]. \tag{3.21}$$

The dispersion coefficient can be approximated by, $D_z = w_g(z)R$, proportional to the speed of the eddies acting to disperse material and the length scale of these eddies. The diameter of plumal eddies will be limited by the lateral length scale of the plume, the radius, R. The rate of change of the mass of particle with respect to time and change in mass flux per unit height can be written (as seen without the dispersive flux in Equation (3.8)) equal to the source and sink terms seen in the fallout/re-entrainment mechanism,

$$\frac{\partial m_p}{\partial t} + \frac{\partial}{\partial z}\left[q_{mp} - AD_z \frac{\partial \rho_p}{\partial z}\right] = P\rho_p \left(k_R E(w_g) - w_s \frac{\partial R}{\partial z}\right) \tag{3.22}$$

3.3 Alternative models

In addition to the conservation equations discussed above, there are some particle models that have been developed describing fallout as a function of atmospheric and eruptive conditions. From a mathematical point of view there are very good reasons why one might proceed in such a way. The introduction of variables relating to ash particles directly to the gaseous conservation equations leads to increased coupling of the equations, that is co-dependence, as well as (most importantly) non-linearity for the particles. This in turn prevents the superposition of solutions and requires all particle classes to be run simultaneously through a single simulation, thereby increasing the difficulty of implementation and computational cost. However, with this increased complexity it is hoped that more nuanced phenomena of plumes can be explored. The following models are included for curiosity's sake, but they are

taken no further than this chapter as they lack the desired underpinning of a mechanistic fallout.

3.3.1 The Suzuki Distribution (1983)

A commonly used model for particle fallout was derived by Suzuki (1983) and is succinctly expressed by McKibbin (2008). Given as a release density distribution $\zeta(z)$ with units $\left[\frac{kg}{kg\,m}\right]$ it can be expressed as,

$$\zeta(z) = \frac{A^2}{H_{max}\left[1 + (A-1)\exp(-A)\right]}\overline{W}\exp\left[-A\overline{W}\right]. \tag{3.23}$$

A is known as the Suzuki constant, H_{max} the maximum plume height and $\overline{W} = \frac{w_g(z)}{w_g(0)}$ a dimensionless velocity profile. This profile can then be normalised to the initial particle flux. Both Suzuki (1983) and McKibbin (2008) consider a simple velocity profile,

$$w(z) = w(0)\left(1 - \frac{z}{H}\right)^{\lambda}, \tag{3.24}$$

where λ is a real number which both papers go on to take as 1; this gives $\overline{W} = \left(1 - \frac{z}{H}\right)$.

3.3.2 Continuous particle size and neutral buoyancy fallout - Sparks *et al.* (1997 - Chapter 4, page 101-105)

Sparks *et.al.* (1997) also considered the distribution of particle diameter within the plume assuming a Gaussian distribution, denoted here as S, and explicitly written,

$$S(L_p) = \frac{1}{\sqrt{2\pi}L_p\sigma_\phi}\exp\left(-\frac{(\log_2(L_p) - \mu_\phi)^2}{2\sigma_\phi^2}\right) \tag{3.25}$$

where μ_ϕ and σ_ϕ are the logarithmic mean and log-normal variance respectively of the particle diameter. Particles are then considered 'lost' when they can no-longer be suspended by the advecting gas. Defining $L_{p,max}$ to be the maximum particle diameter that has a positive

vertical velocity in the plume, the mass flux of particles is given by:

$$q_{mp} = \sigma_p A_e w_e \int_0^{L_{p,max}} S(l) dl. \tag{3.26}$$

This changes according to,

$$\frac{dq_{mp}}{dz} = \sigma_p A_e w_e S(L_{p,max}) \frac{d}{dz}\Big[\, L_{p,max}\Big]. \tag{3.27}$$

Such a distribution represents a very useful description of continuous particle fallout, and rests on a reasonably sound assumption (Neutral buoyancy fallout). However, should one wish to investigate the transport of a specific subset of particles of discrete length scales, such a distribution produces a discrete fallout profile and in doing so limits the potential of the model.

Chapter 4

Internal Dynamics

In this chapter, we will describe a few final features of the plume before setting up our conservation equations for the liquid water, ice, and gaseous components of a plume. The few outstanding details concern the states of water, the plume radius, and a thorough look at the velocities of plumal elements. Ultimately this prepares us to derive the remaining conservation equations which dominate the plume dynamics.

4.1 Qualitative model

As a plume passes through the atmosphere there is a shear force applied between the two gaseous bodies and as a result atmospheric gas will be drawn into the plume as it rises and energy is dispersed in the acceleration and heating of these entrained gases. Simultaneously there is a force applied to the plume as a result of the buoyancy of its constituent elements which causes further changes in its speed. The effects of this entrainment of mass, conversion of energy and application of force can be modelled in conservation equations for the mass, energy and momentum. In applying these principles of conservation the following shows the derivation of the corresponding mathematical equations.

To simplify the modelling process we have made assumptions (already mentioned) that allow the plume variables to be modelled as functions of altitude and time alone, with the column standing symmetrically about the central vertical axis. In spite of the large scales

on which volcanic plumes exist, the curvature of the earth is neglected, and our $z-$axis is taken perpendicular to a flat horizontal plane. The dependent variables with which we are most concerned are,

Mass of CO_2	:=	m_c	kg m^{-1}
Mass of Dry Air	:=	m_a	kg m^{-1}
Mass of Water Vapour	:=	m_v	kg m^{-1}
Mass of Liquid Water	:=	m_l	kg m^{-1}
Mass of Frozen Water	:=	m_f	kg m^{-1}
Total Mass of Water	:=	m_w	kg m^{-1}
Mass of Particles in class j	:=	m_{pj}	kg m^{-1}
Plume Velocity	:=	w_g	m s^{-1}
Particle Velocity of class j	:=	w_{pj}	m s^{-1}
Particle Latency of class j	:=	w_{sj}	m s^{-1}
Plume Temperature	:=	T	K
Plume Radius	:=	R	m.

The plume can be divided into six components: three gaseous groups and three non-gaseous. Dry volcanic gases, denoted by the subscript c, are largely made up of carbon dioxide; water vapour is denoted by the subscript v; and dry atmospheric gases of which the plume is initially devoid, subscript a. In addition to this we consider the state of water in the plume as the temperature and pressure vary. This means that there is potential for both liquid water (l) and ice (f) to form within the plume. The final component of the plume is volcanic/magmatic/ash particles that are suspended within the rising gas. The particle component, in full generality, can take further subdivisions for different chemical structures of the magma as well as size and shape of the particles but, in the formation of these equations, only classification by particle size is considered. Each of these components have various physical and chemical properties made use of in the modelling.

In brief, the particle latency is the difference between the gas and particle velocities. A more in-depth explanation of this distinction is made in section 4.4.

Because the pressures a plume operates over are not particularly high ($p_{atm} < 101325$ [Pa]), we have assumed throughout the modelling process that all of the gases both inside and out of the plume act as ideal gases, obeying the ideal gas law for air in Equation (2.14). Each component will have a specific heat capacity and each of the non-gaseous components is assumed to have a fixed density (possibly densities for sub-groups of particles).

4.2 Equations of state for water

In the lower reaches of a plume the vented gases can exceed 90% water vapour. This will be diluted in ascension as the specific humidity of the atmosphere will not be of this order and so entrainment will significantly affect this ratio. However within our model water is never lost from the plume and so the total mass flow of water in its various forms will be monotonically increasing. Furthermore plume dynamics immediately after venting play a significant role in the viability of a plume. Therefore in this region water makes up the majority of the plume and has the potential to be highly significant. The term 'viability' regarding a plume indicates the potential for it to achieve and maintain a sustained column.

With vent temperatures of the order of $500 - 1000$ K water will be superheated steam (vapour) before condensing to liquid or depositing as ice. The consideration here is the pressures at which these transitions occur. For simplicity the possibility of water existing in all three states simultaneously will be ignored. In reality this event must occur (assuming vapour condenses and then the temperature crosses the triple point $T_{3w} = 273.16$ [K]). However without considering the effects of inhomogeneity within the plume it would be disingenuous to claim any meaningful results caused specifically by this phenomenon.

Considering the equations of state for water we can determine a bound on the partial pressure of water vapour within the plume, where the partial pressure of water vapour is given, using the molar fraction by,

$$p_v(z) = \frac{n_v}{n_g} p_{atm}(z); \tag{4.1}$$

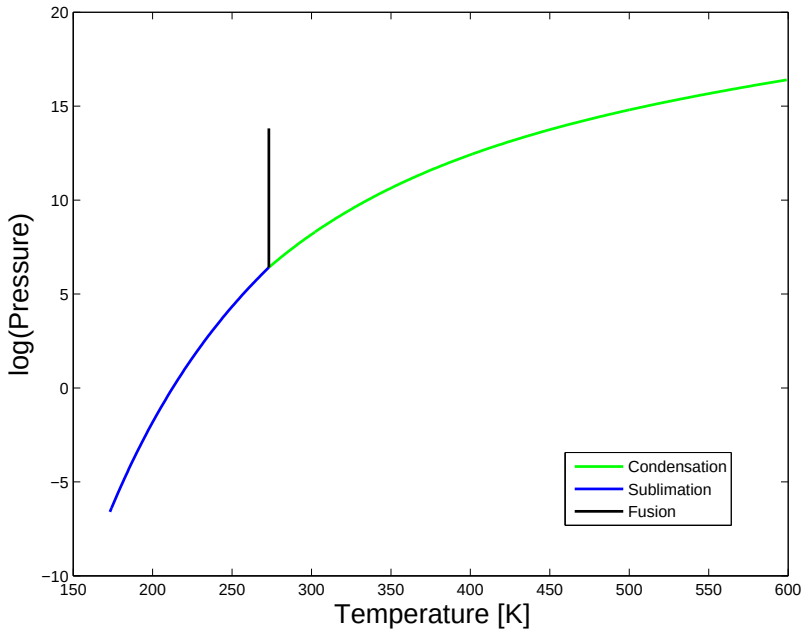

Figure 4-1: The phase-space diagram for water with the condensation line (green), sublimation line (blue), and the freezing line (black).

where $n_\diamond$ represents the number of moles per unit height of the subscripted component. The curves limiting the partial pressure are the condensation and sublimation lines and are taken from standardised steam tables illustrated in Figure 4-1. Assuming that the eruption occurs at or above sea level (submarine eruptions ignored) then the pressure of the plume under our decompression assumption will be bounded by one atmosphere. The partial pressure of water vapour has the plume's total pressure as an upper bound. Nomenclature varies for these curves and so for clarity sake, we define the saturation line of water to be that at which a volume of gas is saturated over either liquid water or ice,

$$p_{v,sat}(T) = \begin{cases} p_{con}(T) & ; \text{ if } T > T_{3w} \\ p_{sub}(T) & ; \text{ if } T < T_{3w} \\ p_{3w} = 101325 \text{ [Pa]} & ; \text{ if } T = T_{3w} \end{cases} \tag{4.2}$$

where p_{con} is the pressure at which a volume of pure water vapour will begin to form condensate, also known as the dew point; p_{sub} is the sublimation pressure at which solid ice will sublimate or conversely water vapour deposit to ice; and p_{3w} is the pressure at the triple point.

With this function defined we can simply say that the partial pressure of water vapour will be at most the saturation pressure for the given temperature. Supposing the partial pressure of water vapour is below the saturation point, then we will assume that all of the water contained in the plume sublimates or evaporates and can rewrite Equation (4.1) as,

$$p_v = \frac{n_w}{n_g} p_{atm}. \tag{4.3}$$

If not then the system is saturated and we can say,

$$p_v = p_{v,sat}(T). \tag{4.4}$$

More concisely this can be expressed as,

$$p_v(z) = \min \left[\frac{n_w}{n_g} p_{atm}(z) \ , \ p_{v,sat}(T) \right]. \tag{4.5}$$

Having the partial pressure of water vapour then allows one to calculate the mass of water vapour within the given volume by the re-arrangement,

$$\begin{aligned} p_v &= \frac{n_v}{n_g} p_{atm} && (4.6) \\ n_v &= \frac{p_v}{p_{atm}} (n_c + n_a + n_v) && (4.7) \\ n_v \left(1 - \frac{p_v}{p_{atm}} \right) &= \frac{p_v}{p_{atm}} (n_c + n_a) && (4.8) \\ n_v &= \frac{p_v}{p_{atm} - p_v} (n_c + n_a) && (4.9) \\ m_v &= n_v M_{H_2O}. && (4.10) \end{aligned}$$

Equations (4.6)−(4.9) are superfluous if we already know $n_v = n_w$. Any additional water mass must therefore either condense to liquid water or be deposited as solid ice, obeying the sum,

$$m_l + m_f = m_w - m_v. \tag{4.11}$$

Away from the triple point, liquid water and ice will not coexist, which can be expressed mathematically as,

$$m_l \, m_f = 0. \tag{4.12}$$

Equations (4.11) and (4.12) may seem to be unnecessary comments, coming directly from the definitions of the variables. However, it is important to note them down to ensure we have enough equations to account for the number of unknown variables.

4.3 Radius calculation

As the plume rises, several factors will affect its lateral expansion. The radius is increased by falling pressure and the entrainment of new gas. The radius is decreased by falling temperature, particle fallout and the condensation or deposition of water. In the conservation of mass flux, rapid changes in component velocities can also have significant effects on the radius.

Stepping away from the rate at which our plume will change in space and time, taking instantaneous values of the dependent variables, one can calculate the volume that the mass contained in a thin section of plume would occupy. The volume of gases are given in the ideal gas equation $p \, dV_\diamond = n_\diamond dz \, R_0 T$, and the volume of solid and liquid components are given as $V_\diamond = \frac{m_\diamond \, dz}{\sigma_\diamond}$, where $\sigma_\diamond$ is the intrinsic density of a component. Note that $m_\diamond$ represents the mass of a material per unit height in the plume and so $m_\diamond \, dz$ is mass of component $\diamond$ in a slice of plume dz metres deep. From these relations, the volume of a section of plume dV can be written,

$$dV = \frac{n_g \, dz R_0 T}{p_{atm}} + \frac{m_f dz}{\sigma_f} + \frac{m_l dz}{\sigma_l} + \frac{m_p dz}{\sigma_p}. \tag{4.13}$$

The number of moles of gas in the section, $n_g\ dz$, is a variable misleadingly simple in appearance. Expanding $n_g\ dz$ to its constituent parts gives,

$$\begin{aligned} dV &= (n_c + n_a + n_v)\frac{R_0 T}{p_a tm} + \frac{m_f dz}{\sigma_f} + \frac{m_l dz}{\sigma_l} + \frac{m_p dz}{\sigma_p} && (4.14) \\ &= \left(\frac{m_c dz}{M_{CO2}} + \frac{m_a dz}{M_{atm}} + \frac{m_v dz}{M_{H2O}}\right)\frac{R_0 T}{p_a tm} + \frac{m_f dz}{\sigma_f} + \frac{m_l dz}{\sigma_l} + \frac{m_p dz}{\sigma_p} && (4.15) \\ & && (4.16) \end{aligned}$$

The thickness of our arbitrary slice is a common factor in each term so we can remove it to give a reasonable differential equation for the volume of the plume.

$$\frac{dV}{dz} = \left(\frac{m_c}{M_{CO2}} + \frac{m_a}{M_{atm}} + \frac{m_v}{M_{H2O}}\right)\frac{R_0 T}{p_a tm} + \frac{m_f}{\sigma_f} + \frac{m_l}{\sigma_l} + \frac{m_p}{\sigma_p}. \quad (4.17)$$

However this does not quite provide the radius, which is the variable we are concerned with here, the issue being that we are yet to formally describe the shape of the plume. Locally a plume slice can be approximated to look like a partial cone as seen in Figure 4-2, the volume of which can be expressed as:

$$\begin{aligned} dV &= \frac{\pi dz}{3}\left(R^2 + (R + dR)R + (R + dR)^2\right) && (4.18) \\ &= \frac{\pi dz}{3}\left(3R^2 + 3RdR + dR^2\right) && (4.19) \end{aligned}$$

Given the angle of the plume edge to the horizontal, ϑ, dR can be expressed as, $dR = \frac{dz}{\tan(\vartheta)}$. Taking the limit as the height of our section goes to zero sends $dR \to 0$, and expresses the volume derivative as a function of the radius.

$$\begin{aligned} \lim_{dz \to 0} \frac{\pi}{3}\left(3R^2 + 3RdR + dR^2\right) &= \pi R^2 && (4.20) \\ \frac{dV}{dz} &= \pi R^2. && (4.21) \end{aligned}$$

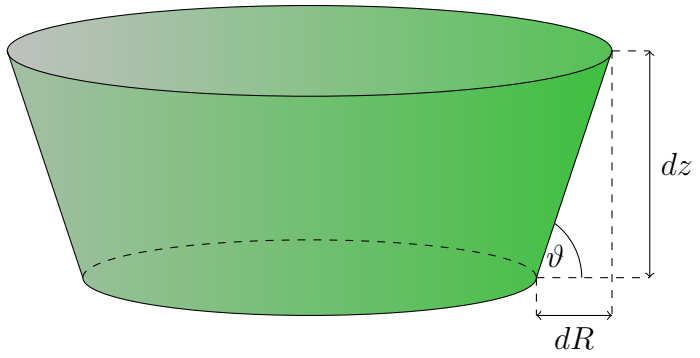

Figure 4-2: An arbitrarily thin section of plume with circular cross-section and constant slope.

This gives us a relation between the mass contained in a section of plume and the radius,

$$\frac{dV}{dz} = \left(\frac{m_c}{M_{CO2}} + \frac{m_a}{M_{atm}} + \frac{m_v}{M_{H2O}}\right)\frac{R_0 T}{p_a tm} + \frac{m_f}{\sigma_f} + \frac{m_l}{\sigma_l} + \frac{m_p}{\sigma_p} \tag{4.22}$$

$$R = \sqrt{\frac{1}{\pi}\frac{dV}{dz}}. \tag{4.23}$$

4.4 Velocity components

One of the more significant variations in the model presented here when compared to those in the literature review is the distinction of the speed of the gaseous and water components of the plume to that of the volcanic particles. At this stage any liquid water or ice is assumed to travel at the gas speed. The four non-zero velocity components (all orientated with the z axis) are,

$$\begin{aligned} w_g(z) &:= \text{Gas speed} \\ w_p(z) &:= \text{Particle speed} \\ w_s(z) &:= \text{Particle latency} \\ w_T(z) &:= \text{Terminal latency} \end{aligned}$$

The gas speed is the average speed of the gas within the plume at altitude z; similarly the particle speed is the average speed of particles in the plume at altitude z. The particle

latency is the difference between the gas velocity and the particle velocity $w_s = w_g - w_p$, often called the settling speed; however to avoid confusion between the particle latency, the settling speed and the terminal latency, this distinction is made. The sign of the particle latency corresponds to the sign of the drag force (acting on particles) orientated positively with the z axis. The terminal latency of a particle, as considered here, does not necessarily bear any relation to the actual particle velocity. The terminal latency represents the value of particle latency expected for the drag force to equal the weight. These forces are, for the most part, not balanced within the plume until particles reach their point of neutral buoyancy where $w_p(z_{NB}) = 0$.

As discussed in the preliminaries, seen in Equation (2.7), particle acceleration can be expressed mathematically as,

$$w_p \frac{dw_p}{dz} = a_p = \frac{F_g + F_D}{\mu_p}, \tag{4.24}$$

where forces are taken as,

$$\begin{aligned} F_g &= -\mu_p g & (4.25)\\ F_D &= \frac{1}{2}\rho_g w_s |w_s| C_D A_p. & (4.26) \end{aligned}$$

for C_D the drag coefficient, and A_p, the cross sectional area of a particle. We have assumed that all drag on particles is equal to the drag seen on a particle with velocity w_p deposited in linear flow with velocity w_g ignoring any possible nuances of drag in an eddy. The implications this holds, and details regarding the drag coefficient can be seen in Section 2.5. Given the density of a particle σ_p we can re-write the above equations,

$$\begin{aligned} w_p \frac{dw_p}{dz} &= a_p & (4.27)\\ &= \frac{-\mu_p g + \frac{1}{2}\rho_g w_s |w_s| C_D A_p}{\mu_p} & (4.28)\\ &= \left(-g + \frac{\frac{1}{2}\rho_g w_s |w_s| C_D \pi L_p^2}{\frac{4}{3}\pi L_p^3 \sigma_p} \right) & (4.29)\\ &= \left(-g + \frac{3}{8}\frac{\rho_g}{\sigma_p}\frac{C_D}{L_p} w_s |w_s| \right). & (4.30) \end{aligned}$$

Given the gas and particle velocities, the particle latency is immediate. The terminal latency of particles within a plume is needed for a particular situation in simulations in which particles are retained beyond their point of neutral buoyancy. Particles cannot be advected past this height as it is defined by the altitude at which a particle class has zero velocity. However, with the introduction of a dispersion term, assuming that the particle class has not been entirely lost, particles can be dispersed further. In such a case it is assumed that particles will settle within the plume at their terminal latency, which increases significantly for large particles as atmospheric pressure drops with altitude. The terminal latency of a particle is attained when all of the forces on it are balanced, that is to say, $F_D + F_g = 0$. Where the particle has zero acceleration, $w_s = w_T$, and, from Equation (4.30), we have:

$$w_T|w_T| = \frac{8\sigma_p L_p}{3\rho_g C_D} g \tag{4.31}$$

$$w_g - w_p = \sqrt{\frac{8\sigma_p L_p}{3\rho_g C_D} g} \tag{4.32}$$

$$w_p = w_g - \sqrt{\frac{8\sigma_p L_p}{3\rho_g C_D} g}. \tag{4.33}$$

Regarding liquid water, and ice, it is acknowledged that rain droplets and balls of ice may ultimately be more accurately modelled as particles. However this is a significant complication and requires a model to describe the rate of their formation and size. Considering the complexity this would add to the model and the constraints of the project this element has therefore been left open for future development.

4.5 Conservation equations

The foundations of this model lie in the conservation of mass, momentum and energy. Deriving these under the assumption that the lateral expansion of the plume is negligible we have a general form of the equations. For a given quantity the sum of its rate of change with respect to time and rate of change of flux per unit height will be equal to any source or sink terms. Within the model we are only considering a small number of sources and sinks deemed to be significant. Those are vent emissions, entrainment, particle exchange,

and work done on the plume by the atmosphere.

In this section we go through a rudimentary formulation of Sparks *et al.* (1997) which, under rearrangement, shows similarities to the derivations of McKibbin (2012). Building on the work of McKibbin, we finalise a time-dependent model incorporating the results of the previous chapter, specifically Subsection 3.1.3.

4.5.1 Formulations of Sparks *et al.* (1997)

Considering a sustained eruption, the two driving phenomena are a buoyancy force implicated by a density difference between the plume and atmosphere; and an entrainment law describing the drawing of atmospheric gas into a moving plume.

In the following, the notation used in Sparks *et al.* (1997) has be replaced with the notation outlined at the start of the thesis. After being initially presented true to the original source, the equations are rearranged for mathematical aesthetics and for as much similarity to the work of McKibbin (2012) as possible, supporting the conclusions made Subsection 4.5.2. For specific accreditation the following are attributed to Woods (1988) and Sparks *et al.* (1997).

In the conservation of mass equations the right hand side represents the entrainment of atmospheric gas.

$$\frac{d}{dz}\left[\rho_m w R^2\right] = 2kwR\rho_{atm} \tag{4.34}$$

$$\frac{dq_m}{dz} = 2\pi R\rho_{atm}kw = P\rho_{atm}E(w). \tag{4.35}$$

Following this, conservation of momentum is stated as,

$$\frac{d}{dz}\Big[\rho_m w^2 R^2\Big] = R^2 g(\rho_{atm} - \rho_m) \tag{4.36}$$

$$\frac{d}{dz}\Big[q_m w\Big] = A(\rho_{atm} - \rho_m)g, \tag{4.37}$$

where the right hand side represents a buoyancy force applied by the atmosphere on the plume.

Conservation of enthalpy takes the only gain in energy to be that given by entrained air,

$$\frac{d}{dz}\left[\rho_m w R^2 \left(C_{Pg}T + \frac{w^2}{2} + gz\right)\right] = 2kwR\rho_{atm}(C_{P,atm}T_{atm} + gz) \tag{4.38}$$

$$\frac{d}{dz}\left[q_m \left(C_{Pg}T + \frac{w^2}{2} + gz\right)\right] = \frac{dq_m}{dz}(C_{P,atm}T_{atm} + gz) \tag{4.39}$$

$$\frac{dq_E}{dz} = \frac{dq_m}{dz}(C_{P,atm}T_{atm} + gz). \tag{4.40}$$

The parameters C_{Pg} and $C_{P,atm}$ are the average specific heats at constant pressure within the plume and the atmosphere respectively. The presence of ash particles is acknowledged and within this model assumed to be entirely conserved within the plume. That is, particle mass flux at any altitude is equal to that at eruption.

$$\rho_m w R^2 \frac{m_p}{m_p + m_g} = \rho_{me} w_e R_e^2 \frac{m_{pe}}{m_{pe} + m_{ge}} \tag{4.41}$$

$$\rho_m A \frac{m_p}{m_p + m_g} w = \rho_{me} A_e \frac{m_{pe}}{m_{pe} + m_{ge}} w_e \tag{4.42}$$

$$\frac{m_p(m_p + m_g)}{m_p + m_g} w = \frac{m_{pe}(m_{pe} + m_{ge})}{m_{pe} + m_{ge}} w_e \tag{4.43}$$

$$q_{mp} = q_{mpe}. \tag{4.44}$$

No distinction between different gases in the plume mixture is made and it is assumed that all components of the plume have the same vertical speed, w.

4.5.2 Formulations of McKibbin (2012)

McKibbin (2012) derived similar equations, seen here in the original format, for an established but time-dependent plume. The time dependency here allows for time-dependent emissions or atmospheric conditions, but not expansion from the first explosive event. The significant source and sink terms considered are,

- Entrainment of mass

- Energy held by entrained mass
- Particle fallout
- Energy lost through particle fallout.
- Buoyancy force
- Work done by atmosphere

McKibbin partitions the gas component into three groups and particles into N groups defined by particle size. The gases are assumed to travel with the same speed while distinctions are made for the speed of each particle class. In doing so we have the following equations:

Splitting the mass of plume gases into the three components: volcanic, dry atmosphere and water; entrainment is proportioned by specific humidity,

$$\frac{\partial m_c}{\partial t} + \frac{\partial}{\partial z}\left[m_c w_g\right] = 0 \tag{4.45}$$

$$\frac{\partial m_a}{\partial t} + \frac{\partial}{\partial z}\left[m_a w_g\right] = \frac{1}{1+\omega} P \rho_{atm} E(w_g) \tag{4.46}$$

$$\frac{\partial m_w}{\partial t} + \frac{\partial}{\partial z}\left[m_w w_g\right] = \frac{\omega}{1+\omega} P \rho_{atm} E(w_g). \tag{4.47}$$

Considering several cohorts, $j = 1, 2, ..N$, of particle size and (ignoring particle agglomeration or further fragmentation) equations for conservation of particle mass are introduced. The model describes a situation similar to the total conservation but makes the exception that particles will fall out of the plume at a certain height, z_j, at which the particle speed is zero. That is to say the plume is travelling sufficiently fast for particles to be suspended at that height but not advected any further. This model is given to be,

$$\frac{\partial m_{pj}}{\partial t} + \frac{\partial}{\partial z}\left[m_{pj} w_{pj}\right] = -\delta(z - z_{NB,j}) q_{mpj}, \tag{4.48}$$

as seen in Equation (3.1), with the addition of the index, j.

Conservation of momentum remains unchanged in essence and differs only by the distinction

of particle components and particle speed.

$$\begin{aligned} &\frac{\partial}{\partial t}\left[(m_g+m_l+m_f)w_g+\sum_{j=1}^{N}m_{pj}w_{pj}\right] \\ &+\frac{\partial}{\partial z}\left[(m_g+m_l+m_f)w_g^2+\sum_{j=1}^{N}m_{pj}w_{pj}^2\right] \;=\; A(\rho_{atm}-\rho_m)g. \end{aligned} \tag{4.49}$$

In the same way the enthalpy equation is not radically altered however additional source/sink terms are included to represent the work rate of the buoyancy force and that of the entrained air:

$$\begin{aligned} &\tfrac{\partial}{\partial t}\left[\begin{array}{l}(m_c+m_a+m_w)\left(\frac{1}{2}w_g^2+gz\right)+m_ch_c+m_ah_a+m_wh_w\\ \quad+\sum_{j=1}^{N}m_{pj}\left(\frac{1}{2}w_{pj}^2+h_{pj}+gz\right)\end{array}\right] \\ &+\tfrac{\partial}{\partial z}\left[\begin{array}{l}(m_c+m_a+m_w)\left(\frac{1}{2}w_g^2+gz\right)w_g+(m_ch_c+m_ah_a+m_wh_w)w_g\\ \quad+\sum_{j=1}^{N}m_{pj}\left(\frac{1}{2}w_{pj}^2+h_{pj}+gz\right)w_{pj}\end{array}\right] \\ &=\; A(\rho_{atm}-\rho_m)gw_g+\left[\tfrac{h_{a,atm}+\omega h_{w,atm}}{1+\omega}+gz\right]P\rho_{atm}E(w_g)+Pp_{atm}E(w_g). \end{aligned} \tag{4.50}$$

This is perhaps simpler when in the form,

$$\begin{aligned} &\tfrac{\partial}{\partial t}\left[E_g+E_p\right]+\tfrac{\partial}{\partial z}\left[q_{Eg}+q_{Ep}\right] \\ &=\; A(\rho_{atm}-\rho_m)gw_g+\left[\tfrac{h_{a,atm}+\omega h_{w,atm}}{1+\omega}+gz\right]P\rho_{atm}E(w_g)+Pp_{atm}E(w_g) \end{aligned} \tag{4.51}$$

From here we do indeed have a strong foundation for the model but, for a few minor alterations. Describing the final form of all of the conservation equations we arrive with the set of equations seen below.

4.5.3 Derivations of the finalised conservation equations

Considering the flow of mass across the plume boundary conserving mass in our model is relatively straight forward. The gases in our plume define the size of the plume as we work our way up the column and so by definition no gas can be lost. Volcanic gas is only added

at eruption as an initial condition. Therefore the flux of these gases does not change,

$$\frac{\partial m_c}{\partial t} + \frac{\partial q_{mc}}{\partial z} = 0 \tag{4.52}$$

At eruption there is no atmospheric gas present. There is only dry volcanic gas and water vapour. However as the plume passes through the stationary atmosphere gas is entrained. The concentration flux at any point on the boundary is given as the product of the atmospheric density, ρ_{atm}, and the entrainment speed, $E(w_g)$. Integrating about the plume perimeter gives:

$$\frac{\partial m_g}{\partial t} + \frac{\partial q_{mg}}{\partial z} = P\rho_{atm}E(w_g). \tag{4.53}$$

This must then be split between dry atmospheric gas and water vapour according to the specific humidity (ω),

$$\frac{\partial m_a}{\partial t} + \frac{\partial q_{ma}}{\partial z} = \frac{1}{1+\omega}P\rho_{atm}E(w_g) \tag{4.54}$$

$$\frac{\partial m_w}{\partial t} + \frac{\partial q_{mw}}{\partial z} = \frac{\omega}{1+\omega}P\rho_{atm}E(w_g) \tag{4.55}$$

Equations (4.53)−(4.55) are seen in the previous subsection, and listed (4.45)−(4.47).

Chapter 3 provides an in depth look at particle exchange on the boundary of a plume. Incorporating internal vertical dispersion, particle fallout, and re-entrainment we derived Equation (3.22). Generalised this equation for N distinct particle classes the relationship can be expressed,

$$\frac{\partial m_{pj}}{\partial t} + \frac{\partial}{\partial z}\left[q_{mpj} - AD_z\frac{\partial \rho_{pj}}{\partial z}\right] = P\rho_{pj}\left(k_{Rj}E(w_g) - w_{sj}\frac{\partial R}{\partial z}\right). \tag{4.56}$$

Momentum is given by mass times speed $p = mv$ and is conserved under the addition of mass via entrainment however is affected by the buoyancy force placed on the plume by the

atmosphere. The rate of change of momentum equals any force applied to it giving equation,

$$\begin{aligned} &\frac{\partial}{\partial t}\left[(m_g+m_l+m_f)w_g+\sum_{j=1}^{N}m_{pj}w_{pj}\right] \\ +&\frac{\partial}{\partial z}\left[(m_g+m_l+m_f)w_g^2+\sum_{j=1}^{N}m_{pj}w_{pj}^2\right] \;=\; A(\rho_{atm}-\rho_m)g. \end{aligned} \tag{4.57}$$

This result is attributed to McKibbin (2012) in the previous subsection, in Equation (4.49).

The significant forms of energy in a plume are kinetic $\frac{1}{2}m_\diamond w_\diamond^2$, potential $m_\diamond gz$, and thermal $m_\diamond h_\diamond$. Energy is lost and gained along with mass as components pass into and out of the plume. In this model heat is not conducted nor radiated from the plume nor is friction within the plume or friction on the plume boundary considered significant. The work done by the atmosphere on the plume is seen qualitatively in the momentum equation, referenced (4.49), and applied as a work rate in the energy equation. The following result is not identical to Equation (4.66) as there is a separation seen here between work done to the gaseous components and work done to the particle cohorts all of which have different velocities.

$$\begin{aligned} \frac{\partial E}{\partial t}+\frac{\partial q_{Eg}}{\partial z}+\left(\sum_{j=1}^{N}\frac{\partial q_{Epj}}{\partial z}\right) \;=\; & F_g w_g+\left(\sum_{j=1}^{N}F_{pj}w_{pj}\right) \\ & +(gz+h_{a,atm})\left[\frac{\partial m_a}{\partial t}+\frac{\partial q_{ma}w_g}{\partial z}\right] \\ & +(gz+h_{w,atm})\left[\frac{\partial m_w}{\partial t}+\frac{\partial q_{mw}w_g}{\partial z}\right] \\ & +\sum_{j=1}^{N}\left(\frac{E_{pj}}{m_{pj}}\right)\left[\frac{\partial m_{pj}}{\partial t}+\frac{\partial q_{mpj}w_{pj}}{\partial z}\right], \end{aligned} \tag{4.58}$$

where for compactness sake we have,

$$q_{E\diamond} \;=\; q_{m\diamond}\left(\frac{1}{2}w_\diamond^2+gz+h_\diamond\right) \tag{4.59}$$

$$F_g \;=\; A(\rho_{atm}-\rho_m)g-F_p. \tag{4.60}$$

4.5.4 Time-Dependent Model summary

Summarising the set of equations in our final model gives the following list:

$$\frac{\partial m_c}{\partial t} + \frac{\partial}{\partial z}\left[m_c w_g\right] = 0 \tag{4.61}$$

$$\frac{\partial m_a}{\partial t} + \frac{\partial}{\partial z}\left[m_a w_g\right] = \frac{1}{1+\omega} P \rho_{atm} E(w_g) \tag{4.62}$$

$$\frac{\partial m_w}{\partial t} + \frac{\partial}{\partial z}\left[m_w w_g\right] = \frac{\omega}{1+\omega} P \rho_{atm} E(w_g) \tag{4.63}$$

$$\frac{\partial m_{pj}}{\partial t} + \frac{\partial}{\partial z}\left[q_{mpj} - A D_z \frac{\partial \rho_{pj}}{\partial z}\right] = P \rho_{pj}\left(k_{Rj} E(w_g) - w_{sj}\frac{\partial R}{\partial z}\right) \tag{4.64}$$

$$\begin{array}{l} \frac{\partial}{\partial t}\left[(m_g + m_l + m_f) w_g + \sum_{j=1}^{N} m_{pj} w_{pj}\right] \\ + \frac{\partial}{\partial z}\left[(m_g + m_l + m_f) w_g^2 + \sum_{j=1}^{N} m_{pj} w_{pj}^2\right] = A(\rho_{atm} - \rho_m) g \end{array} \tag{4.65}$$

$$\begin{array}{l} \frac{\partial}{\partial t}\left[\begin{array}{l} (m_c + m_a + m_w)\left(\frac{1}{2} w_g^2 + g z\right) + m_c h_c + m_a h_a + m_w h_w \\ \quad + \sum_{j=1}^{N} m_{pj}\left(\frac{1}{2} w_{pj}^2 + h_{pj} + g z\right) \end{array}\right] \\ + \frac{\partial}{\partial z}\left[\begin{array}{l} (m_c + m_a + m_w)\left(\frac{1}{2} w_g^2 + g z\right) w_g + (m_c h_c + m_a h_a + m_w h_w) w_g \\ \quad + \sum_{j=1}^{N} m_{pj}\left(\frac{1}{2} w_{pj}^2 + h_{pj} + g z\right) w_{pj} \end{array}\right] \\ = A(\rho_{atm} - \rho_m) g w_g + \left[\frac{h_{a,atm} + \omega h_{w,atm}}{1+\omega} + g z\right] P \rho_{atm} E(w_g) + P p_{atm} E(w_g) \end{array} \tag{4.66}$$

$$w_p \frac{\partial w_p}{\partial z} = -g + \frac{3}{8}\frac{\rho_g}{\sigma_p}\frac{C_D}{L_p} w_s |w_s| \tag{4.67}$$

$$w_s = w_g - w_p \tag{4.68}$$

$$\pi R^2 = \frac{\partial V}{\partial z} \tag{4.69}$$

$$m_w = m_v + m_l + m_f \tag{4.70}$$

$$p_v = \min\left[\frac{n_w}{n_g} p_{atm}\ ,\ p_{v,sat}\right] \tag{4.71}$$

$$m_l\, m_f = 0 \tag{4.72}$$

Chapter 5

Steady-Flow Model and Solutions

In this section we present a numerical solution to our steady-flow model of an established and sustained, buoyant plume. By this we mean the solution to the set of equations presented in the final section of the previous chapter taken with the following assumptions:

- The eruption in question exists with relatively constant vent output and atmospheric conditions for a sufficiently long period of time that it can be considered in steady state and modelled independent of time, t. This corresponds to a steady flow and is represented mathematically by setting all time derivatives in the previous section to zero, $\frac{\partial}{\partial t} \equiv 0$. In this we have the further implication that for the plume to reach a steady state it must be considered both established and sustained.

- The eruption in question under the preceding assumption is not in a steady-state corresponding to a low altitude collapsed fountain leading to a sustained pyroclastic flow. The eruption has been sufficiently forceful that an ash cloud is produced with a region in which its density is less than the surrounding atmosphere and expands a significant distance from the original vent altitude. This is a qualitative assumption on the actual plume. The model listed in Section 4.5.4 is deterministic and if there is a buoyant plume for a given set of vent conditions then the model will simulate the buoyant plume.

What follows is a list of the variables we are concerned with, a set of initial conditions which are defined by approximations made for the plume's vent conditions as well as the list of

equations used to model the plume. Details of various parameters used are listed in the final section of this chapter.

5.1 Key variables

In order for the independent variables to be sufficiently determined we require an equivalent number of equations to dictate their behaviour as there are variables themselves. Aside from altitude, z, acting as our one independent variable, we have twelve dependent variables considered in the model, as outlined in Table 5.1. This is not a unique set of dependent

Table 5.1: The dependent variables used in the Steady-Flow Model of an established and sustained, buoyant plume

Variable	Notation	Units
Mass of CO_2	m_c	kg m^{-1}
Mass of Dry Air	m_a	kg m^{-1}
Mass of Water Vapour	m_v	kg m^{-1}
Mass of Liquid Water	m_l	kg m^{-1}
Mass of Frozen Water	m_f	kg m^{-1}
Total Mass of Water	m_w	kg m^{-1}
Mass of Particles	m_p	kg m^{-1}
Plume Velocity	w_g	m s^{-1}
Particle Velocity	w_p	m s^{-1}
Particle Latency	w_s	m s^{-1}
Plume Temperature	T	K
Plume Radius	R	m

variables and the system can be described by a distinct set. Furthermore, within Table 5.1, the total mass of water is indeed the sum of the mass of its three constituent elements,

$$m_w = m_v + m_l + m_f. \tag{5.1}$$

These four variables are included, in lieu of a subset of three of them, because of the simplifications this allows in the differential equations without the need for further clarification of this relationship.

5.2 Boundary conditions

The following list of boundary conditions are intended to be indicative of a general volcanic eruption.

Total Gas Flux	:=	q_{mge}	=	2.0×10^7	kg s^{-1}
Flux of Water	:=	q_{mwe}	=	$0.95 \times q_{mg}$	kg s^{-1}
Flux of CO_2	:=	q_{mce}	=	$0.05 \times q_{mg}$	kg s^{-1}
Flux of Dry Air	:=	q_{mae}	=	$0.00 \times q_{mg}$	kg s^{-1}
Particle Concentration	:=	ρ_{pe}	=	0.3	kg m^{-3}
Particle Concentration Gradient	:=	$\frac{d\rho_{pe}}{dz}$	=	0	kg m^{-4}
Particle Latency	:=	w_{se}	=	w_T	m s^{-1}
Plume Temperature	:=	T_e	=	1000	K
Plume Radius	:=	R_e	=	200	m.

If we assume that particles are at their terminal velocity within the gas flow as they are vented out of the conduit then boundary conditions for the remaining variables can be derived from these. The total gas flux is indeed a linear combination of the three constituent gases however in expressing the conditions in this way the initial distribution of mass is more clearly displayed.

At the given temperature, according to our water state relations, we know that all of the water content will be vapour.

$$q_{mve} = q_{mwe} \tag{5.2}$$

$$q_{mle} = 0 \tag{5.3}$$

$$q_{mfe} = 0. \tag{5.4}$$

Given the vent radius, R_e, the vent's cross sectional area, when approximated to be circular, is given as $A_e = \pi R_e^2$. From this, given the total flow through the vent the gas velocity can

be determined:

$$\begin{aligned} p_{atm}(dV - dV_p) &= \frac{m_{ge}dz}{M_{ge}} R_0 T_e \\ p_{atm}\left(\frac{dV}{dz} - \frac{dV_p}{dz}\right) &= \frac{q_{mge}}{w_{ge}M_{ge}} R_0 T_e \\ p_{atm}\left(\pi R_e^2 - \frac{\rho_{pe}}{\sigma_p}\pi R_e^2\right) &= \frac{q_{mge}}{w_{ge}M_{ge}} R_0 T_e \\ w_{ge} &= \frac{q_{mge} R_0 T_e}{M_{ge} p_{atm} \pi R_e^2}\left(\frac{\sigma_p}{\sigma_p - \rho_{pe}}\right). \end{aligned} \tag{5.5}$$

Note that M_{ge}, is the average molar mass of the gas mixture at venting, and R_0 is the universal gas constant, unrelated to the radius. From the model equations we have the particle speed,

$$w_{pe} = w_{ge} - w_{se}. \tag{5.6}$$

5.3 Steady-Flow Model summary

We can simplify the equations of Subsection 4.5.4 to describe a steady flow plume. The possibility of partitioning particles into several classes exists, however the computational machinery developed during the project does not have this capability and so all particles are approximated to be of the same size and grouped into a single cohort.

$$\frac{d}{dz}\left[m_c w_g\right] = 0 \tag{5.7}$$

$$\frac{d}{dz}\left[m_a w_g\right] = \frac{1}{1+\omega} P \rho_{atm} E(w_g) \tag{5.8}$$

$$\frac{d}{dz}\left[m_w w_g\right] = \frac{\omega}{1+\omega} P \rho_{atm} E(w_g) \tag{5.9}$$

$$\frac{dq_{mp}}{dz} - \frac{d}{dz}\left[D_z \frac{d\rho_p}{dz}\right] = P\rho_p\left(k_R E(w_g) - w_s \frac{dR}{dz}\right) \tag{5.10}$$

$$\frac{d}{dz}\left[q_{mg} w_g + q_{mp} w_p\right] = A(\rho_{atm} - \rho_m)g \tag{5.11}$$

$$
\begin{aligned}
\frac{d}{dz}\left[\begin{array}{l}
\frac{1}{2}(m_c+m_a+m_w)w_g^3+\frac{1}{2}m_p w_p^3 \\
\quad +(m_c h_c+m_a h_a+m_w h_w)w_g+m_p h_p w_p \\
\quad\quad +(m_c+m_a+m_w)gzw_g+m_p gzw_p
\end{array}\right] & \\
= \left(A(\rho_{atm}-\rho_m)g-m_p a_p\right)w_g+m_p a_p w_p & \\
+\left[\frac{h_{a,atm}+\omega h_{w,atm}}{1+\omega}+gz\right]P\rho_{atm}E(w_g)+Pp_{atm}E(w_g) & \\
-(\frac{1}{2}w_p^2+h_p+gz)\left[P\rho_p\left(k_R E(w_g)-w_s\frac{dR}{dz}\right)\right] &
\end{aligned}
\tag{5.12}
$$

$$
\begin{aligned}
w_p\frac{\partial}{\partial z}[w_p] &= \frac{1}{2}\frac{w_s^2 C_D\rho_g}{\sigma_p L_p}-g && (5.13)\\
w_s &= w_g-w_p && (5.14)\\
\pi R^2 &= \frac{d}{dz}\left[V_c+V_a+V_w+V_p\right] && (5.15)\\
m_w &= m_v+m_l+m_f && (5.16)\\
p_v &= \min\left[\frac{n_w}{n_g}p_{atm}\ ,\ p_{v,sat}\right] && (5.17)\\
m_l\ m_f &= 0. && (5.18)
\end{aligned}
$$

Equation (5.13) describes the general dynamic of particle speed. In Section 4.4 we have discussed the event of particle dispersion beyond the neutral buoyancy of a particle class. In such a case we take the alternate equations,

$$
\begin{aligned}
w_s &= \sqrt{\frac{8\sigma_p L_p}{3\rho_g C_D}g} && (5.19)\\
w_p &= w_g-w_s, && (5.20)
\end{aligned}
$$

where particles settle at their terminal latency. In addition to this, should the re-entrainment rate exceed the extrainment rate, then the fallout is taken to be zero in accordance with Equation (3.20).

5.4 Numerical method and structuring

The computer program created to solve the above equations does not rely on particularly complex numerical methods. The system of differential equations have been algebraically rearranged and written in terms of derivatives of both the essential dependant variables and various miscellaneous variables used for simplicity. Discretising the problems domain with a constant step size, $\triangle z$, we have then integrated forward by the Euler method. Suppose that a state of the system $\mathbf{x}$, has a know derivative, $\frac{d\mathbf{x}}{dz} = \mathbf{f}(\mathbf{x})$ then, we can approximate the next spatial step by,

$$\mathbf{x}^{(i+1)} = \mathbf{x}^{(i)} + \mathbf{f}^{(i)} \times \triangle z, \tag{5.21}$$

5.5 Solutions

Simulating the model allows for a range of comparisons to be made. In this section we highlight a few interesting facets of plume behaviour which feature for a range of initial conditions. In the following simulation, in addition to parameters outlined in Table 5.2, the diameter of particles is taken to be uniformly $L_p = 1 \times 10^{-3}$ m or 1 mm. Variation in L_p is explored subsequently. The profile shown in Figure 5-1 in isolation shows a rather straightforward, and entirely expected result. Whilst there is considerable disparity between atmospheric and plumal temperatures, the plume will rapidly cool; the rate of change in temperature slows considerably when the disparity is less pronounced. This effect would be magnified with the introduction of radiative terms. When we pair the temperature profile with the ambient air pressure we get a rather more interesting result.

Following the path of the partial pressure of water vapour in Figure 5-2(a), as the temperature drops we see an intersection with the sublimation line which becomes a limiting factor on the partial pressure. This phenomenon is seen simultaneously in Figure 5-2(b) as the water vapour begins to deposit as ice at an altitude of just over 10 km. Under different eruptive conditions, the changes in water distribution can also be seen with an intersection

on the condensation line which often continues to fall until the triple point is crossed where we see the condensate freeze to ice. If it seems odd that in Figure 5-2(b) solid water (ice) is forming within a volcanic plume we must keep in mind that this is several kilometers above the vent. A considerable amount work has been done entraining atmospheric gas which removes energy from the plume. Furthermore, atmosphere being largely cooler than the plumal gas acts to further reduce the temperature as it is mixed into the plume.

Plume deceleration, seen in Figure 5-7, causes the largest variations in the water mass distribution diagram (Figure 5-2(b)). When gas is flowing into regions faster than it is out, a considerable amount of mass will accumulate. This is particularly evident in the bottom and top 6 km of the plume. It would appear then, that entrainment has a negligible affect on the mass of water in the plume. However, entrainment is a significant cause in the deceleration of the plume in the bottom 6 km.

In Figure 5-3 the umbrella region is clearly identifiable and coincides with the rapid deceleration of gases seen in Figure 5-7 from 12 km. Above 17 km, we see the plume radius tend to infinity; this is an artificial facet of the model. Because the solution is integrated until the plume gases lose all kinetic energy, under the conservation of flux, as the gas speed goes to zero, the mass of the various components per unit height tends to infinity. In generating a steady state solution, we are strictly considering the plume structure as time goes to infinity in the time dependent case. This in turn corresponds to an infinite volume of gas being transported (from vent emission and entrainment) to the apex of the plume and hence our infinite volume. It is obviously not our intention to say that Plinian eruptions attain infinite radius in the umbrella region, merely that this is the limiting case of a sustained eruption. The introduction of a sufficiently strong cross wind to the model, could remove this issue and represent a more realistic upper boundary of the plume.

Figures 5-4, 5-5, and 5-6, describe the resultant particle transport in the simulation. In Figure 5-5 we can begin by noting the lack of particle loss prior to 4km from the vent. Near the base of the plume, the volcanic gasses are travelling at a considerable velocity which

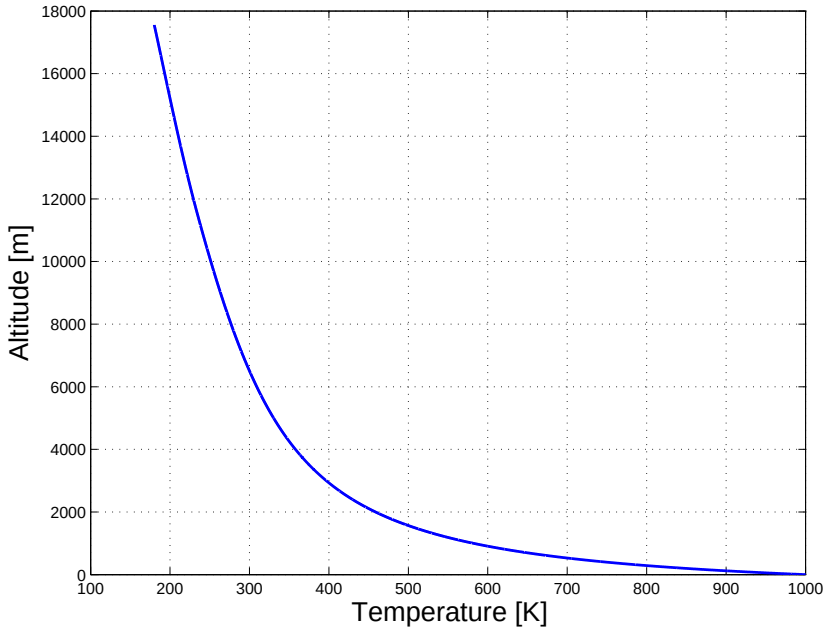

Figure 5-1: The plume's temperature [K] against altitude.

results in very high entrainment rates. This makes for a highly significant reentrainment rate which prevents any loss. However, as the plume slows, so do entrainment rates and we begin to see particles exiting the plume permanently. In Figure 5-4 we see a decaying concentration of particles in the plumes ascension. This is a result of particle loss and the particle-free atmospheric gas that is entrained. This decay does not carry over to the mass of particles per unit height in Figure 5-6 as the infinite plume radius at the apex dominates this dynamic. Running time dependent simulations would remove this facet however they stand, the results give a good indication of the interaction between particles.

A most interesting result, is seen in Figure 5-7. In the first 1.5 km of the plume the particles are travelling faster than the gases which at first seems to be counter-intuitive. However, if particles are to be decelerated on reasonable time-scales this is indeed a necessary facet of the model. The argument follows that immediately after venting, gravitational acceleration alone will not decelerate particles faster than the deceleration experienced by gases. This is seen in the dashed blue line of Figure 5-7 which shows particles under the influence of gravity alone travelling at high speeds considerably longer than the plume gasses. Therefore under the assumption that the only forces acting on particles are weight and aerodynamic drag, the

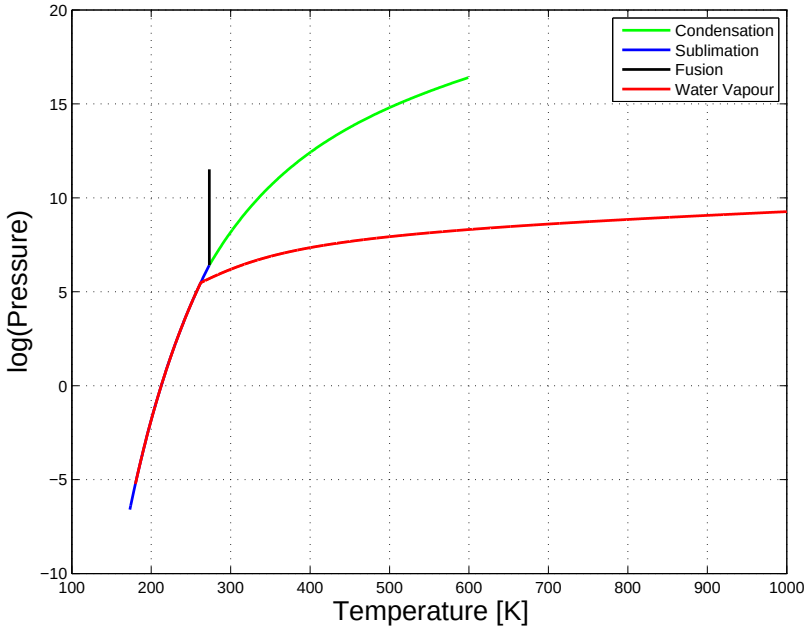

(a)

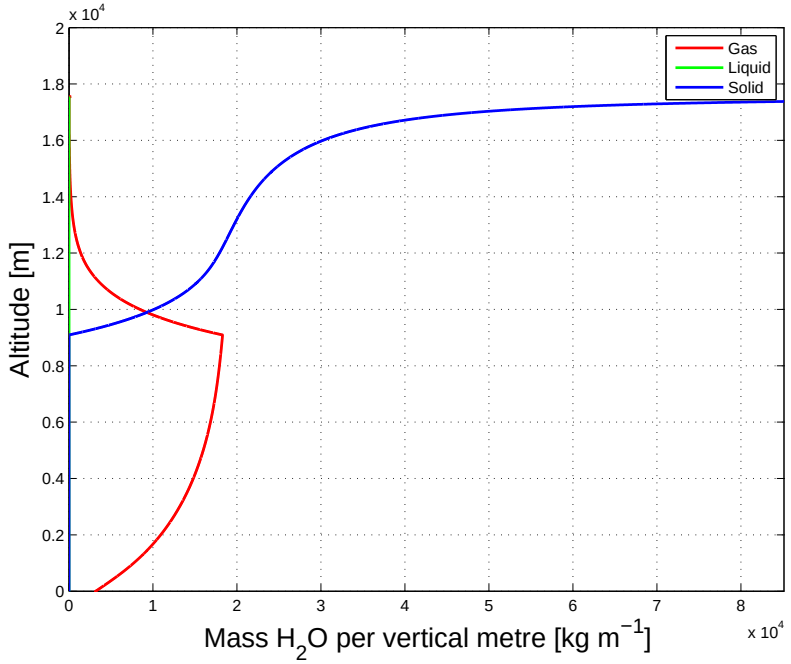

(b)

Figure 5-2: (a) The partial pressure of water vapour (red), superimposed onto the water phase-space diagram. (b) The change in the mass distribution of water as the plume rises into the atmosphere.

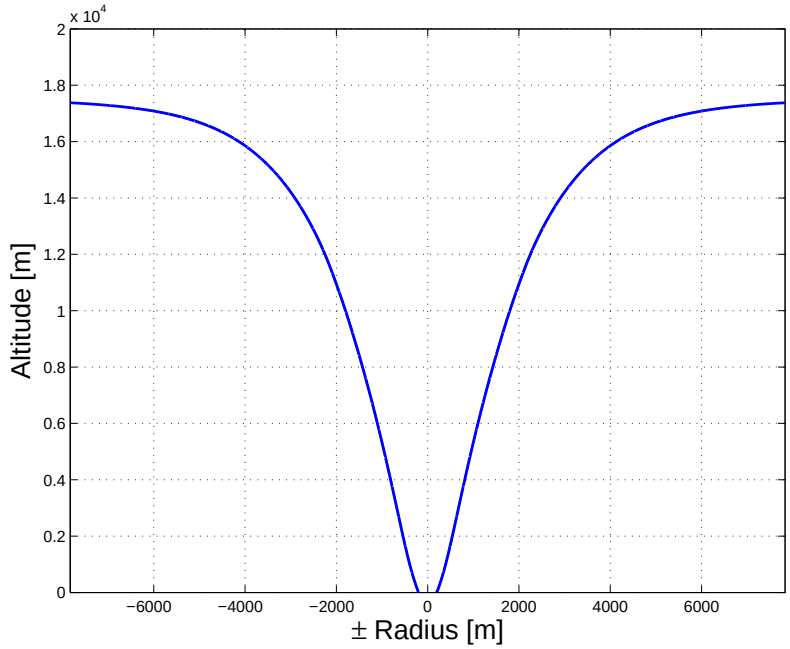

Figure 5-3: Vertical plume cross section.

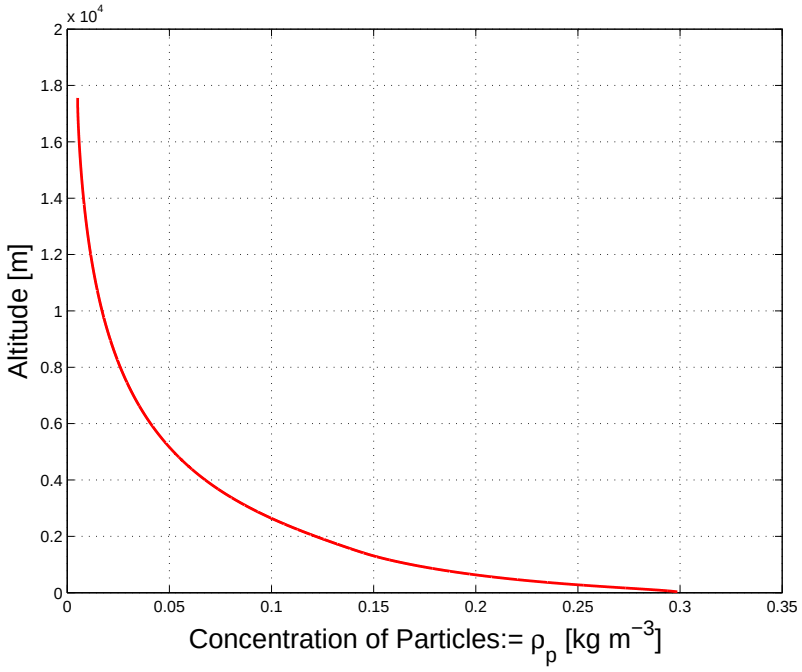

Figure 5-4: The concentration of particles in the plume against altitude.

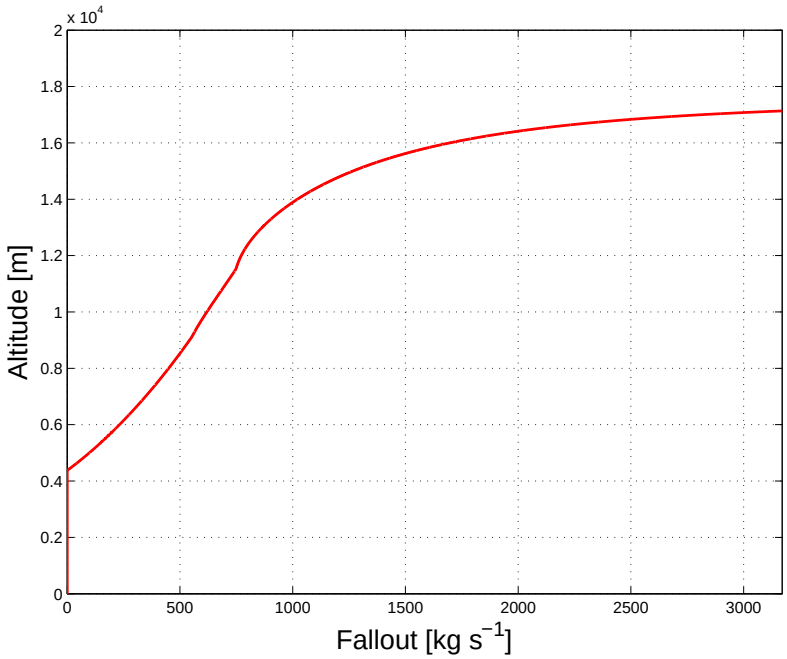

Figure 5-5: The rate of fallout of particles (red) in [kg s^{-1}] against altitude.

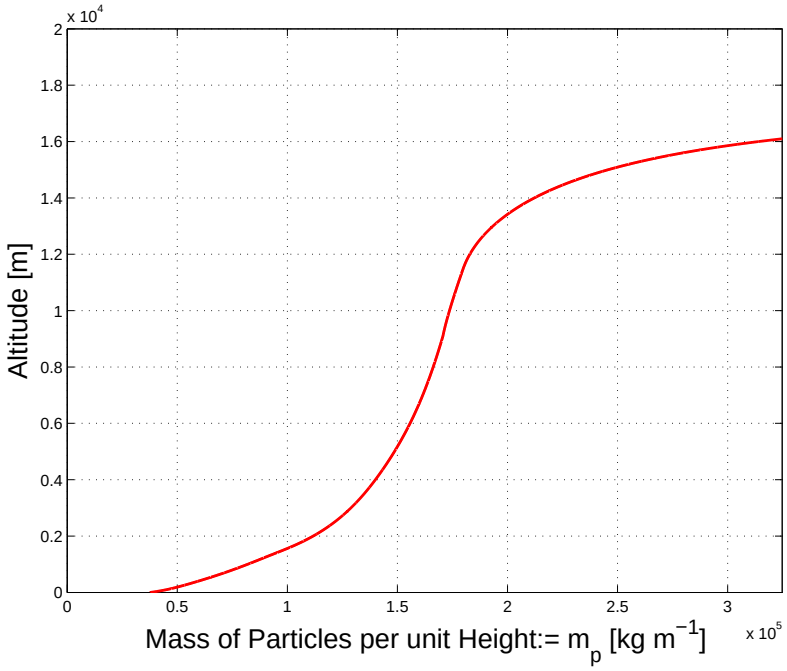

Figure 5-6: The mass of particles per unit height against altitude

drag force must account for a considerable component of the deceleration if particles are to maintain a speed even similar to the gases. If particles are, on average, going to experience this downward drag force then they must, on average, be travelling faster than the gases which they are expected to be decelerated by. Therefore, for a brief period of time particles are travelling faster than the plume gasses causing greater deceleration as a result of the drag force.

In terms of the time-scales of transport across the full height of the plume, in Chapter 2 we have an estimation from the Brunt-Viäsälä frequency that for a Plinian eruption this timescale ought to be of the order 2 to 3 minutes. Integrating over the height of the simulated plume,

$$\int_0^{z_L} \frac{dz}{w_g} \simeq 2.011 \times 10^2, \tag{5.22}$$

we have a total travel time of 200 seconds which is indeed of such an order.

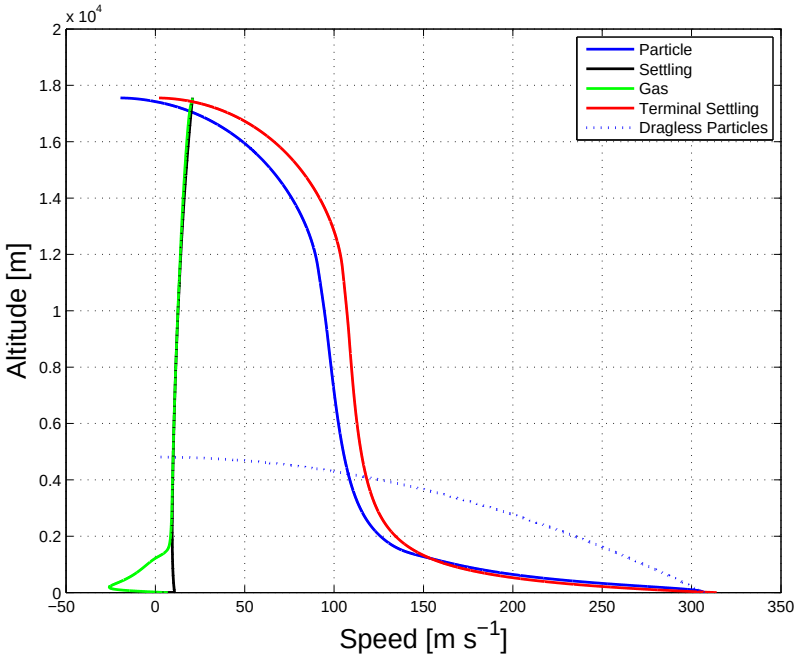

Figure 5-7: The profiles of various measured speeds against altitude. The dashed blue line represents the trajectory of particles in the absence of drag

With the same boundary conditions, as outlined in Table 5.2, it is worth exploring variation in the radius of particles and the effect this has on the particle profiles. Running the simulation with a single particle class, consecutively setting $L_p \in \{0.25, 1, 4, 16\}$ mm, we can explore a range of fallout profiles ranging from suspended particles through to those beginning to display ballistic trajectories. The results are plotted in Figure 5-8. For the first two particle classes, $L_p = 0.25$ mm and $L_p = 1$ mm, we can clearly see particle fallout, and therefore the presence of particles, through to the apex of the plume. This is a clear example of the drag force exerted by re-entrainment dominating any settling due to gravity, which is key in the classification of suspended particles. For particles with $L_p = 4$ mm, and $L_p = 16$ mm, fallout can be seen from near the base of the plume. For $L_p = 4$ mm particles are retained for a distance beyond the initial peak of particle loss signifying some, albeit limited, characteristics of suspension. However, for the large 16 mm particles, the drag force is insufficient to transport any particles to such heights, indicating that particles of this size represent a ballistic categorisation. This is in line with the division made by Sparks *et al.* (1997) limiting suspended particle classification at 1 mm. Considering ballistic particles takes us beyond the intended scope of the model. The features in this model are limited in focus to consider suspended particles. As we begin to discuss ballistic particles the angle at which the particles leave the vent as well as other factors will have lasting effects on the fallout rate around the vent. This is not to say that the results seen in Figure 5-8 are without merit as they provide a clear indication as to the limits of the model and even in describing the loss of large particles they provide an approximation for the fallout.

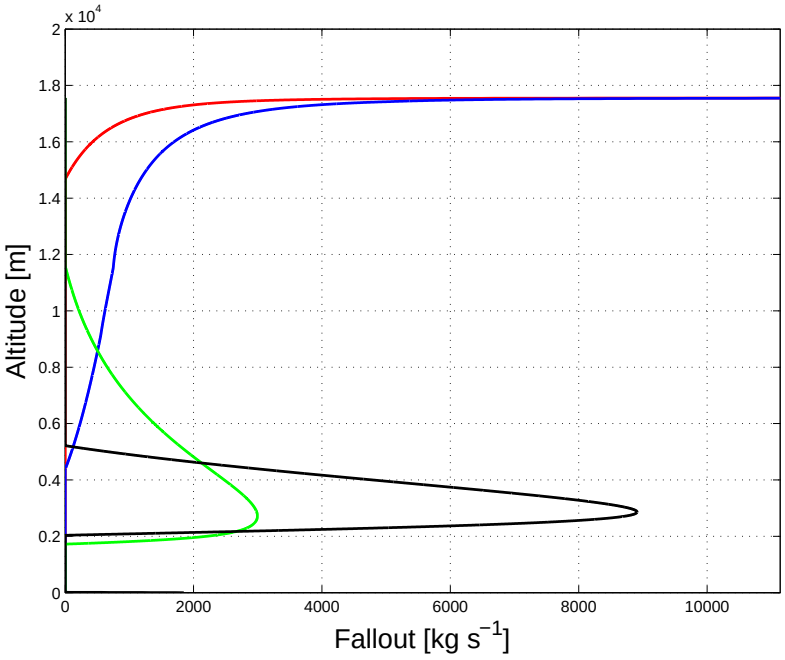

Figure 5-8: Fallout profiles for particles with diameters of 0.25 mm (red), 1.00 mm (blue), 4.00 mm (green), and 16.00 mm (black).

Table 5.2: Parameter set used to generate figures 5-2 through 5-8.

Parameter	Notation	Value	Units
Molar mass of Water	M_{H_20}	0.0200	kg mol^{-1}
Molar mass of CO_2	M_{CO_2}	0.0441	kg mol^{-1}
Molar mass of Dry atmospheric gas	M_{atm}	0.0290	kg mol^{-1}
Universal Gas Constant	R_0	8.314	J mol^{-1} K^{-1}
Density of Liquid Water	σ_l	998.0	kg m^{-3}
Density of Ice	σ_f	920.0	kg m^{-3}
Specific Heat Capacity of Dry Atmospheric Gas at constant pressure	c_{pa}	1.050×10^3	J kg^{-1} K^{-1}
Specific Heat Capacity of CO_2 at constant pressure	c_{pc}	1.000×10^3;	J kg^{-1} K^{-1}
Specific Heat Capacity of Water Vapour at constant pressure	c_{pv}	1.860×10^3;	J kg^{-1} K^{-1}
Specific Heat Capacity of Liquid Water	c_{pl}	4.210×10^3;	J kg^{-1} K^{-1}
Specific Heat Capacity of Ice	c_{pf}	2.050×10^3;	J kg^{-1} K^{-1}
Specific Heat Capacity of Ash Particles	c_{pp}	1.617×10^3	J kg^{-1} K^{-1}
Gravitational Acceleration	g	9.807	m s^{-2}
Intrinsic Ash Density	σ_p	2.500×10^3	kg m^{-3}
Drag coefficient of Ash particles	C_D	1.084	-
Average Mass of a single Ash Particle	μ_p	$\frac{4}{3}L_p^3\sigma_p$	kg
Spatial step size	$\triangle z$	1	m

Chapter 6

Conclusions

6.1 Summary

The aim of this thesis was to present a compilation of mathematical models seen in various literature sources, as well as new material produced through analysis of the literature. Beginning in publications by Sparks et al. (1997) and McKibbin (2012) we have built up a simple model focussing on the effects of entrainment and particle exchange.

A great deal of assumptions have been made in the modelling process. The most significant assumptions made in the modelling process were:

- The plume is vented as a mixture of carbon dioxide and water only.
- Thin, horizontal cross-sections of the plume can be approximated as partial cones, with smooth surfaces.
- The plume's velocity profile can be considered 'top-hat' which is to say invariant across horizontal cross-sections of the plume. In addition to this, turbulence within the plume is sufficient to approximate a well mixed plume across horizontal cross-sections.
- The atmosphere is sufficiently sedate that wind and other time dependant atmospheric variations are inconsequential to the structure of the column.

- Particles are dispersed vertically according to Fick's law with a length scale of eddies corresponding to the radius of the plume.

- Particles are considered to be spherical and have a fixed density across all clast sizes. From here, the drag on particles is taken proportional to the particle latency squared with the length scale of the Reynolds number corresponding to the diameter of a particle.

- Water within the plume changes state strictly according to condensation, sublimation, freezing lines given in a standard phase-state diagram.

- When solved, the vent emissions have been taken to remain constant for a sufficiently long period time that the column can be considered to be in steady flow.

After simplifying our equations to represent a steady flow plume we presented sufficient boundary conditions and caveats to simulate a Plinian eruption until such a height that the gaseous advection is exhausted. To solve the system of ordinary differential equations, that made up the model presented in section 5.3, we discretised the plume's central vertical axis into 1 m high steps and integrated the solution up from a boundary condition on the vent. This integral has been calculated within a custom written computer package developed in the MATLAB environment.

6.2 Analysis

We have managed to compile aspects of mathematical models for volcanic plumes from a variety of sources and having built upon them written a system of ordinary differential equations for which we can now generate numerical solutions from arbitrary initial conditions. Under the assumptions outlined at the beginning of chapter 5 the research objective has been accomplished. In affirmation of our solutions we see a great deal of behaviour expected of buoyant plumes discussed previously in the literature including the generation of an umbrella region and a distinctive velocity profile characteristic of Plinian eruptions.

6.3 Further Work

The study of volcanic plumes remains an exciting field and the results of this thesis by no means represent a complete picture of their dynamics. Throughout the modelling process we have had a great deal of extensions in mind, far more than could have possibly been achieved within the time frame of the project. To mention a few of these avenues, we look forward to the advancement of this model in the following directions:

- The results shown in this thesis are limited to a single particle class per numerical solution. In wielding the full capability of the analytical model we hope to see machinery incorporating multiple particle classifications, in a single simulation.

- Again our full analytical model is expressed with time-dependent terms present, and so solving the full time-dependent equations would be an interesting advancement of the results, in particular with a focus on the transition between two distinct states of steady flow in an eruption.

- Beyond the existing scope of the model presented, investigation into fountain or plume collapse with the hope of incorporation into a time-dependent solution would be a valuable addition to the understanding of plumes.

- Including multiple particle classes is limited within this model to suspended particles. Modelling the behaviour of large ballistic particles immediately after venting would be a useful step towards relaxing assumptions on the plume content. For early plume fallout of ballistic particles and rocks, the inclusion of decompression dynamics surrounding the vent is an important consideration.

- The concatenation of either this or more complex plume models to atmospheric dispersion models to simulate the full range of particle transport from venting through fallout to the depositing of particles at ground level.

- Plumes are often seen drifting away from a central cartesian axis over the vent as a result of cross-winds in the atmosphere. Incorporating more detailed atmospheric

conditions, particularly the affects of cross winds, will allow results to more accurately reflect real world events.

- As mentioned in the results, as the plume nears its apex, the top-hat approximation may begin to break down. Further investigation into the limits of this assumption and possible inclusion of Gaussian velocity profiles will give a more natural shape to the plume and possibly increase the level of accuracy at large distances from the vent.

- The drag coefficient of particles is highly influential on their fallout profiles. More detailed models for the shape of particles and the corresponding drag coefficients would be an interesting component to incorporate into the model.

- Further modelling done on the transition between states of water, in particular the size and rates of growth for water droplets and hail stones. In doing so it is hoped that non-vapour water velocities can be considered and the extrainment of water considered in a similar manner to the particles. Included in this subproblem of plumes is particle conglomeration and post-vent fracturing as liquid water and ice play a significant role in the adhesive properties of ash.

Bibliography

Batchelor, G.K., *An introduction to fluid dynamics*, Cambridge University Press, London, 1967.

Bursik, M.I. (1989) Effects of the drag force on the rise height of particles in the gas-thrust region of volcanic eruption columns. *Geophysical Research Letters* 16, 441-444.

Bursik, M.I. and Woods, A.W. (1991) Buoyant, superbuoyant and collapsing eruption columns, *Journal of Volcanology and Geothermal Research* 45, 347-350.

Bursik, M.I., Sparks, R.S.J., Carey, S.N. and Gilbert, J.S. (1994) The Concentration of ash in volcanic plumes inferred from dispersal data. *Proceedings of the First International Symposium on Volcanic Ash and Aviation Safety US Geological Survey Bulletin* 2047, 19-29.

Bursik, M.I., Sparks, R.S.J., Gilbert, J.S. and Carey, S.N. (1992b) Sedimentation of tephra by volcanic plumes: I Theory and its comparison with a study of the Fogo A plinian deposit, Sao Miguel (Azores). *Bulletin of Volcanology* 54, 329-344.

Bursik, M., Carey, S. and Sparks, R.S.J. (1992a) A gravity current model for the May 18, 1980 Mount St. Helens plume. *Geophysical Research Letters* 19, 1663-1666.

Carey, S.N. and Sigurdsson, H. (1985) The May 18, 1980 eruption of Mount St, Helens 2. Modeling of dynamics of the plinian phase . *Journal of Geophysical Research*, 90, 2948-2958.

Carey, S.N. and Sigurdsson, H. (1986) The 1982 eruptions of El Chichon volcano, Mexico (2): Observations and numerical modelling of tephra fall distribution. *Bulletin of Volcanology*, 48, 127-141.

Carey, S.N. and Sigurdsson, H. (1987) Temporal variations in column height and magma discharge rate during the 79 A.D. eruption of Veuvius. *Geological Society of America Bulletin*, 99, 303-314.

Carey, S.N. and Sigurdsson, H. (1989) The intensity of plinian eruptions. *Bulletin of Volcanology*, 51, 28-40.

Carey, S.N. and Sparks, R.S.J. (1986) Quantatative models of fallout and dispersal of tephra from volcanic eruption columns. *Bulletin of Volcanology*, 48, 109-125.

Carey, S.N., Sigurdsson, H. and Sparks, R.S.J. (1988) Experimental studies of particle-laden plumes. *Journal of Geophysical Research*, 93, 15314-15328

Carey, S.N., Gardner, J., Sigurdsson, H. and Criswell, W. (1990) Variations in column height and magma discharge during the May 18, 1980 eruption of Mount St, Helens. *Journal of Volcanology and Geothermal Research*, 43, 99-112.

Champion, K.S.W., Cole, A.E., Kantor, A.J., Chapter 14: Standard and Reference Temperatures. In A.S. Jursa & M. Tschirch (Eds.), *Handbook of Geophysics and the Space Environment*. Springfield, Virginia, Air Force Geophysics Laboratory, Air Force Systems Command, United States Airforce, 1985.

Earth Science and Remote Sensing Unit, NASA Johnson Space Center (2006). ISS013E24184 Mount Cleveland. Retrieved from http://commons.wikimedia.org/wiki/File:ISS013E24184_Mount_Cleveland.jpg

Fischer, H.B. (1979) Turbulent jets and plumes. In: Fischer, H.B., List, E.J., Koh, R.C.Y., Imberger, J., Brooks, N.H., (eds) *Mixing in Inland and Coastal waters*. Academic Press (San Diego, California), pp. 315-389.

Green, D.W., and Perry, R.H., *Perry's chemical engineers' handbook* (8th ed.), McGraw-Hill, New York, 2008.

Halmer, M.M., Schmincke, H.-U., and Graf, H.-F. (2002) The annual volcanic gas input into the atmosphere, in particular into the stratosphere: a global data set for the past 100 years. *Journal of Volcanology and Geothermal Research*, 115, 511-528.

Harper, S.A., Mathematical models for dispersal of aerosol droplets in an agricultural setting, PhD thesis, Massey University, New Zealand, 2008.

Harris, D.M., Rose, Jr, W.I., Roe, R., Thompson, M.R., Radar observations of ash eruptions. In: Lipman, P.W., Mullineaux, D.R., (eds) *The 1980 Eruptions of Mount St. Helens, Washington.*Washington D.C., United States Government Printing Office, 1981.

Kaminski, E., Tait, S. and Carazzo, G. (2005) Turbulent entrainment in jets with arbitrary buoyancy. *Journal of Fluid Mechanics*, 526, 361-376.

Kharioutdinov, M.F., Randall, D.A. (2003) Cloud resolving modeling of the ARM summer 1997 IOP: Model formulation, results, uncertainties, and sensitiviteis, *J. Atmos. Sci.*, 60, 607-625.

Mastin, L.G. (2007), A user-friendly one-dimensional model for wet volcanic plumes, *Geochem. Geophys. Geosys.*, 8, Q03014, doi:10.1029/2006GC001455.

McKibbin, R., Mathematicl modelling of aerosol transport and deposition: Analytic formulae for fast computation. M. Sànchez-Marrè, J. Béjar, J. Comas, A. E. Rizzoli, G. Guariso (Eds.). Proceedings of the iEMSs Fourth Biennial Meeting: International Congress on Environmental Modelling and Software (iEMSs 2008). International Environmental Modelling and Software Society, Barcelona, Catalonia, July 2008.

McKibbin, R. (2012) Mathematical modelling of volcanic plumes: Part 1 [Private Correspondence]. Auckland, New Zealand: Massey University, Centre for Mathematics in Industry.

McKibbin, R. (2012) Mathematical modelling of volcanic plumes: Part 2 [Private Correspondence]. Auckland, New Zealand: Massey University, Centre for Mathematics in Industry.

Morton, B.R., Taylor, G.I. and Turner, J.S. (1956) Gravitational turbulent convection from maintained and instantaneous sources. *Proceedings of the Royal Society of London Series* A234, 1-23.

Pfeiffer, T., Costa, A., Macedonio, G., (2005) A model for the numerical simulation of tephra fall deposits. *Journal of Volcanology and Geothermal Research*, 140, 273-294.

Portland State Aerospace Society (2004) A Quick Derivation relating altitude to air pressure. Retrieved from
http://psas.pdx.edu/RocketScience/PressureAltitude_Derived.pdf

Solovitz, S. A., and L. G. Mastin (2009) Experimental study of near-field air entrainment by subsonic volcanic jets, J. Geophys. Res., 114, B10203,
doi:10.1029/2009JB006298.

Sparks, R.S.J., (1986) The dimensions and dynamics of volcanic eruption columns. *Bulletin of Volcanology*, 48, 3-15.

Sparks, R.S.J., Wilson, L. (1982) Explosive volcanic eruptions – V. Observations of plume dynamics during the 1979 Soulfière eruption, St. Vincent. *Geophysical Journal of the Royal Astronomy Society*, 69, 551-570.

Sparks, R.S.J., Bursik, M.I., Carey, S.N., Gilbert, J.S., Glaze, L.S., Sigurdsson, H. and Woods, A.W., *Volcanic Plumes*, Wiley, New York, 1997.

Suzuki, T. (1983) A theoretical model for dispersion of tephra. *In:* Shimozuru, D. and Yokoyama, I. (eds), *Arc volcanism, physics and tectonics*, Terra Scientific, Tokyo, 95-113.

U.S. Geological Survey (1980). Mount St Helens Eruption - 1980.
Retrieved from http://www.flickr.com/photos/usgeologicalsurvey/11707592844/

Wilson, L., Walker, G.P.L. (1986). Explosive volcanic eruptions - V.I. Ejecta dispersal in plinian eruptions: the control of eruption conditions and atmospheric properties. *Geophysical Journal of the Royal Astronomy Society* 89, 657-679.

Woods, A.W. (1988) The dynamics and thermodynamics of eruption columns. *Bulletin of Volcanology* 50, 169-191

Woods, A.W. (1993) Moist convection and the injection of volcanic ash into the atmosphere. *Journal of Geophysical Research* 98, 17627-17636

Woods, A.W., Bower, S.M. (1995). The decompression of volcanic jets in a crater during explosive volcanic eruptions. *Earth and Planetary Science Letters*, 131, 189-205.